Identification of cracks in thick beams with a cracked beam element model

Identification of cracks in thick beams with a cracked beam element model

Chuanchuan HOU, Yong LU *

Institute for Infrastructure and Environment, School of Engineering, the University of Edinburgh, Edinburgh EH9 3JL, UK

* Correspondence: yong.lu@ed.ac.uk

Abstract

The effect of a crack on the vibration of a beam is a classical problem, and various models have been proposed, ranging from the basic stiffness reduction method to the more sophisticated model involving formulation based on the additional flexibility due to a crack. However, in the damage identification or finite element model updating applications, it is still common practice to employ a simple stiffness reduction factor to represent a crack in the identification process, whereas the use of a more realistic crack model is rather limited. In this paper, the issues with the simple stiffness reduction method, particularly concerning thick beams, are highlighted along with a review of several other crack models. A robust finite element model updating procedure is then presented for the detection of cracks in beams. The description of the crack parameters is based on the cracked beam flexibility formulated by means of the fracture mechanics, and it takes into consideration of shear deformation and coupling between translational and longitudinal vibrations, and thus is particularly suitable for thick beams. The identification procedure employs a global searching technique using Genetic Algorithms, and there is no restriction on the location, severity and the number of cracks to be identified. The procedure is verified to yield satisfactory identification for practically any configurations of cracks in a beam.

Keywords: damage detection; crack; thick beam; cracked beam element; coupling vibration; finite element model updating

1 Introduction

Model-based structural health monitoring and damage identification employ measured vibration data and a structural model to identify the existence, location and severity of damages in the structures. A large amount of research has been published in the last several decades. Several review reports have covered most of the important progress in this area, such as Doebling, et al. [1], Sohn, et al. [2], Fan and Qiao [3], Mottershead and Friswell [4], and Mottershead, et al. [5]. Specialised techniques on the best use of the modal data are continued to be developed (e.g. [6]).

To accurately identify the damage location and severity, it is important to have a sound model for the structure, whether a more detailed finite element (FE) model or a simplified structural model. The model should be capable of representing all important mechanical effects in the structure to reduce the errors in the calculation arising from inadequate modelling considerations. One of the challenges in the modelling for damage identification is the description of damages, or in general terms the choice of the damage parameters.

Damage in a structure is generally localised, thus its effect on the structural response can vary with different loading and deformation conditions. From the structural modelling point of view, the effect of the localised damage can be more comprehensively represented if a detailed continuum FE model is employed. However, a detailed continuum model can hardly be adopted for general damage identification purpose due to the inherent restrictions relating to the damage sensitivity and the limited amount of measurement information. For this reason, simplified models are generally required, and for beam type of structures, the use of beam elements is still common practice.

In a beam component, damage often takes the form of cracks. Several different damage models have been used in previous studies to represent the effect of cracks. Friswell and Penny [7] reviewed the subject of crack modelling for structural health modelling. Generally there are four representative crack models for beams. The first one, which is arguably most widely used, is the local stiffness reduction method. It models the effect of crack by a reduction of the bending stiffness of the cracked beam segment. The second one is the discrete spring model. It divides the cracked beam into different segments at the possible damage locations. The segments are pinned together and rotational springs are added at the damage locations to simulate the remaining bending stiffness. By adjusting the stiffness of the rotational spring, different levels of damage can be simulated. The third approach stems from establishing the local flexibility of the cracked beam in relation to the strain energy release rate. The strain energy can be evaluated with the fracture mechanics. The last approach derives a continuous vibration equation for the cracked beam based on assumed stress and strain fields around the crack area.

An overview of the last three models will be given in Section 2. Herein we shall present an analysis

on the reduced stiffness (or flexural rigidity) method, as it is the simplest method and is still the predominant approach widely used in model updating and damage identification of beams, especially in civil engineering structures. Some of the numerous examples using the reduced stiffness methods can be found in [8-11].

The reduced stiffness method is most often implemented by a reduction of the modulus of elasticity, or the flexural rigidity, for a cracked beam element. In terms of the element stiffness, this means the relationship between the stiffness matrix of a cracked element and the intact element is as follows:

$$K_{\mathrm{e}}^{\mathrm{d}} = \left(1 - D_{\mathrm{e}}\right) K_{\mathrm{e}}^{0} \tag{1}$$

where, $\boldsymbol{K}_{\mathrm{e}}^{0}$ and $\boldsymbol{K}_{\mathrm{e}}^{\mathrm{d}}$ are the element stiffness matrices of the intact and cracked elements, respectively. D_{e} is the parameter which indicates the severity of the crack. D_{e} ranges between 0 and 1; larger D_{e} value means deeper crack in the element.

The implication of the reduced stiffness method is that the stiffness matrix of the cracked element is proportional to that of the intact one. It treats the stiffness reduction as uniform to all degrees of freedom in the cracked element. This can only happen if the actual reduction of the rigidity along the length of the cracked element is uniform. Obviously this is not true in a real cracked beam. The stress will exhibits a concentration at the crack tip and decay rapidly as the location moves away from the crack. As a result, the plane section assumption used in the Euler and Timoshenko beam theories will not be met in the immediate neighbouring region of the crack location. The materials in the vicinity of both sides of the crack will not be stressed and thus contribute little to the stiffness of the section [12].

As a result, using the element stiffness matrix of Eq. (1) will introduce modelling error into the global stiffness matrix of the FE model, which will in turn result in errors in the predicted modal data. The modelling error can sometimes be so large that the element damage severity predicted by this method, which is presented with the parameter D_{e}, could become inconsistent and even contradictory when different sets of modal data are employed. Numerical examples are used to demonstrate this effect in what follows.

A beam with a length to sectional depth ratio (L/B) of 10 is used to demonstrate the problem with the reduced stiffness method, as shown in Fig. 1. Beams of such slenderness are typical in civil engineering structures. The crack is located at $L_{\mathrm{c}} = 0.35L$ from the left end and the crack depth is assumed to be $0.4B$.

To generate the required "measured" modal data for the beam, a refined FE model using continuum solid elements (CPS8R in ABAQUS) is employed to simulate the beam and natural frequencies and mode shapes of the first 6 modes are obtained. The beam is then modelled with Timoshenko beam elements with a high accuracy 3rd order shape function. The Timoshenko beam is discretised into 10

elements of equal length, and the crack is thus incorporated in the 4th element.

There is no simple physical relationship to determine the stiffness reduction factor D_e for the assumed crack. Following the idea of parameter identification, D_e may be determined from an FE model updating process to fit the measured modal data. In the present demonstrative case, there is only one unknown parameter, being the stiffness reduction ratio D_e of the 4th element, to be determined. Therefore one modal frequency is enough for the updating. The first 6 "measured" natural frequencies are used to identify D_e separately. The results are presented in Table 1.

It can be seen that the D_e results based on the first two modes are quite close, around 0.6. It means 60% of the element stiffness is lost due to the crack. However, modes 3 and 4 yield very low D_e values, indicating very light damage. The ratio of the standard deviation to the mean value is as large as 0.592. It means that for the beam with a slenderness ratio of order of 10, which is common in structural engineering applications, no consistent D_e value can be obtained from different modes with the reduced stiffness model.

Upon further check of the mode shapes and the mode shape curvature, which are not shown here, it can be found that for mode 4, the cracked element is at a relatively small curvature location, and this would cause the respective modal properties to be less sensitive to the changes (of stiffness) at the cracked location. However, this is not the case for mode 3, for which the mode shape curvature at the cracked location is relatively high. Therefore, the discrepancy in the equivalent stiffness reductions shown in Table 1 can only be concluded as a result of different stiffness effect of the same physical crack in different modes. That is to say, the usual stiffness reduction approach, whereby a single stiffness reduction factor over a certain element length is employed to represent the effect of a physical crack, is inherently flawed, especially when applied on thick beams under consideration.

A further perspective of the issue with the reduced stiffness approach is demonstrated by performing an updating for an optimized D_e value by the best fit to all of the 6 modes. The D_e value so obtained in this case is 0.635. The modal frequencies with this stiffness factor for the cracked element stiffness are then calculated, and these are compared with the "measured" data in Fig. 2. It can be seen that only mode 1, mode 2 and mode 5 match reasonably well in the results, the 3rd and 4th modes have quite large errors of order of 4-6% in absolute terms with respect to the baseline frequencies.

A seemingly straightforward consideration in improving the situation, still using the stiffness reduction approach, would be to refine the element discretization such that the variation of the stiffness change surrounding a crack could be better represented. However, in a real updating problem where the crack location is not known, this approach would imply an increase by many times the number of unknown parameters, and hence is unlikely to be implementable. Moreover, even with a refined discretization, the result may not turn out to be satisfactory. Herein the same cracked beam

example is used to demonstrate this. We employ Sinha's method [12], which will be discussed in more detail in Section 2. This method describes the stiffness distribution surrounding a crack by a shape function, and so is essentially of similar effect to refining the discretization. The estimated frequency shifts with Sinha's model are shown in Fig. 2. It can be seen that the result has not improved significantly from those using the simple stiffness reduction approach.

The above numerical examples demonstrate that with the reduced stiffness model, inconsistent or conflicting indications of the severity of the crack damage are unavoidable from using data from different modes. Using an optimized procedure could reduce the overall error in matching the modal frequencies collectively, but this procedure does not address the inherent problem that a cracked region in a thick beam cannot be fully represented by a single stiffness reduction factor, consequently the result can still yield large errors in some of the modal frequencies. The implication is that in the inverse damage identification process, in which the crack location is also unknown, and there may be multiple cracks involved, marked errors can result from the use of the stiffness reduction method. To overcome this problem, a more accurate model needs to be considered to represent the crack in a damage identification or model updating application.

The present study has been aimed at developing a robust damage identification approach for cracks in beams, with a special focus on thick beams which present more complexity in terms of the effect of a crack than slender beams. To pave the way for the determination of a beam model which can comprehensively describe the effect of a crack on the vibration properties of a beam, a review of several crack modelling approaches as available from the literature is presented first. The basic formulation of the chosen cracked beam element model is then described. The adequacy of the model is verified in a forward manner by comparing the predicted natural frequencies of the cracked beam with the "actual" results generated from a refined finite element analysis. Subsequently, the cracked beam model is implemented in a general finite element model updating procedure. To tackle the randomness of the crack location, an adaptive process is incorporated, so that the crack is always located around the middle of the beam element containing the crack in the final discretisation. For the updating of the model parameters, we employ the Genetic Algorithms (GA) to perform the searching process. All elements in the beam are subject to the updating for the crack parameters, thus the procedure can be applied in the identification of any location, severity or combination of cracks.

2 Review of existing models for cracked beam

The general influence of cracks on the vibration of beams has been extensively studied in the past, and comprehensive reviews have been published previously (Dimarogonas [13], Friswell and Penny [7]). Most of these studies have been concerned about the vibration formulation for a cracked beam

with known crack parameters, namely location and crack depth, and limited use has been made of these models for inverse crack identification or finite element model updating purposes. In this section, the key considerations and basic modelling outcome of a few representative methods are summarised.

2.1 Models based on stress fields

The presence of a crack in the beam will change the stress and strain fields in the vicinity of the crack. By assuming the stress and strain distributions in this area, the vibration equation of a cracked beam may be established.

Christides and Barr [14] studied the vibration of Bernoulli-Euler beams with one or more pairs of symmetric cracks on both top and bottom sides of the beam. The bending stress in the vicinity of the crack is assumed to decay exponentially from its maximum value at the cracked section to the uncracked value in a certain distance away from the crack. With the assumed stress variation, a vibration function can be obtained for cracked Bernoulli-Euler beams. For a beam with rectangular section, the following function can be obtained:

$$EIQw^{iv} + 2EIQ'w''' + EIQ''w'' + \rho A\ddot{w} = 0 \tag{2}$$

where EI is the bending stiffness of the intact section, ρA is the mass of a unit length, and w is the transverse displacement. Q is an integrated crack function, $Q(x) = \left[1 + C\exp\left(-2\alpha|x - x_0|/d\right)\right]^{-1}$, where $C = I_0/I_d$-1, x_0 is the location of the crack, d is the depth of the section and α is a coefficient obtained from experimental data, which is 0.667 according to Christides and Barr [14].

It can be seen that the above equation is similar to that of the intact Euler beam. The only difference is that an "equivalent" bending stiffness distribution $EIQ(x)$ is used in the function, instead of a constant value EI, as illustrated in Fig. 3.

In Christides and Barr [14], the solution of coefficient α is only against the fundamental natural frequency. Shen and Pierre [15] applied the same theory to evaluate both the natural frequencies and mode shapes of the cracked beam up to the lowest 3 modes. They used a Galerkin-type solution to calibrate the vibration function with finite element modelling results and got a new value for the coefficient α, as 1.936. The same authors then extended the theory to Euler beam with a single-edge crack [16].

Chondros et al. [17] avoided assuming a stress field and established the displacement field in the vicinity of the crack based on Castigliano's theorem and the crack strain energy derived from the fracture mechanics. Once the displacement field is obtained, the strain and stress fields can be calculated, and subsequently a continuous beam vibration equation is established. The method is able

to consider both single-edge and double-edge open cracks.

The above theories only considered bending deformation in the beams. Carneiro and Inman [18] considered shear deformation in the continuous vibration function of cracked beams, extending the crack model to Timoshenko beams. They used a similar bending stress field assumption as in Shen and Pierre [16]. As the shear deformation is involved, they suggested a shear stress disturbance function. The function is based on a quadratic distribution of shear stress along the section depth. Similar to normal stress, the shear stress is assumed to decay exponentially from the crack location with the same decay rate as normal stress.

The developed continuous beam vibration equations can be employed to calculate the natural frequencies and mode shapes of cracked beams, provided that the crack depth and location are known. However, it is not easy to directly employ the continuous vibration equations in damage identification practice, especially when more than one crack is presented in the beams. For damage identification purpose especially when the finite element updating approach is employed, a discretised cracked beam element model need to be developed.

Sinha et al. [12] proposed a cracked Euler-Bernoulli beam element based on Christides and Barr's theory. They simplified the bending stiffness distribution about the crack $EIQ(x)$ to a linear form, as shown in Fig. 3. A cracked beam element can then be formed with the simplified stiffness distribution and cubic shape functions for standard Euler-Bernoulli beam element. In the developed stiffness matrix, the effect of the crack can be modelled with two parameters: the crack depth and the crack location. With the cracked beam element, both forward calculation and damage identification can be carried out. The first advantage of this model is that a "realistic" distribution of bending stiffness surrounding the crack is used and expressed with crack parameters in the model. Therefore in principle both the crack depth and location can be obtained in damage identification. Also, as the crack is described locally with an individual beam element, there is no specific limit on the number of cracks in the beam. Examples of beams with two cracks were given and it was shown that reasonably good damage identification results could be achieved.

It should be noted that in the above model the distribution of the bending stiffness within a cracked beam element is based on an assumed exponential-type stress decay near the crack tip, and the stress decay rate α is obtained by fitting the first natural frequency of experimental cracked beam. Different α values may be obtained if another mode is used in the fitting, as has been shown in Shen and Pierre [15]. Consequently, inconsistent predictions may result for higher modes if the same α value is used, and this is evident from the example shown in Section 1. Moreover, the shear deformation is not included in the model. The example beams used in the original paper [12] had slenderness ratios in the range of 40-70, so the accuracies observed there could not be extended to thicker beams with a

smaller slenderness ratio in terms of the effect of the shear deformation in a cracked beam. Finally, the model does not consider the coupling effect between the longitudinal and transverse modes, which, as will be discussed in Section 3.1, will have important influences in thick beams.

2.2 Methods based on the discrete spring model

This type of methods treats the cracked beam as two segments pinned together at the crack location. A rotational spring is added to the pin to model the effective bending stiffness in the cracked region. A typical discrete spring model is shown in Fig. 4. The stiffness of the spring is related with the depth of the crack and can be obtained with fractural mechanics (Liebowitz, et al. [19]; Okamura, et al. [20]; Ostachowicz and Krawczuk [21]).

The discrete spring model can be used to develop a continuous vibration function for a cracked beam. One representative example is Lele and Maiti [22]. It assumes that the two segments both follow Timoshenko's vibration equations. The rotational stiffness of the spring obtained by Ostachowicz and Krawczuk [21] is used. The boundary conditions at the crack location can be established with the continuity of displacement, moment and shear force, and a jump in the slope which can be calculated with the rotational stiffness of the spring. The global vibration function can then be solved with the boundary conditions at the beam ends and crack location.

By covering the rotational spring element in one element, the model can also be used to develop cracked beam elements, such as the ones developed by Viola et al. [23] and Mehrjoo et al. [24]. In Viola et al. [23], the pinned segments were assumed to follow Timoshenko's theory and described with cubic shape functions. The shape functions were solved with the boundary conditions at the element nodes and crack location. With the shape functions and the unit displacement method, the stiffness matrix for the cracked beam element can be derived. Mehrjoo et al. [24] obtained a Timoshenko-theory based macro element for the cracked beam. They used the superposition principle and unit displacement method to obtain the stiffness matrix for the element without a need to use the shape functions.

Modelling the effect of the crack with a dimensionless spring should be a reasonable assumption if the influence range of the crack is relatively small with respect to the length of the beam (in the continuous vibration theory) or the length of the cracked element (in the macro beam element). Otherwise, using a dimensionless spring to represent the crack effect could introduce larger errors, especially for higher modes. Another problem is that the coupling of longitudinal and transverse vibration in a cracked beam cannot be reflected in the model.

2.3 Cracked beam element based on local flexibility and fracture mechanics

The third approach directly employs the local flexibility brought by the crack to calculate the stiffness

of the cracked beam element. A brief review of this approach, hereinafter referred to as the "cracked beam element" model, is summarized below.

The local flexibility matrix of the cracked beam was initially introduced in the 1980's by Dimarogonas and Papadopoulos [25], and Papadopoulos and Dimarogonas [26] and [27]. According to fracture mechanics, for a cracked structure under a constant load F, the energy release rate G for the crack growth is equivalent to the rate of increase of the total strain energy U_T (Tada, et al. [28]). As a result, the total strain energy of the structure with a crack area A_c will be:

$$U_T = U_0 + U_c \tag{3a}$$

$$U_c = \int_{A_c} G \mathrm{d}A \tag{3b}$$

where U_0 is the strain energy of the intact structure under the constant load, U_c is the additional strain energy brought by the crack, and A_c is the effective crack area.

The energy release rate G can be expressed with the Stress Intensity Factors (SIFs) of the crack as (Tada, et al. [28]):

$$G = \frac{1}{E'}\left(K_I^2 + K_{II}^2 + \frac{1}{1-\nu} K_{III}^2\right) \tag{4}$$

where, K_I, K_{II}, and K_{III} are the stress intensity factors for three different types of cracks, namely opening, sliding and tearing; For plane stress, $E' = E$, and for plane strain, $E' = E/(1-\nu)$, where ν is the Poisson's ratio of the material.

With the total strain energy of the cracked beam, the flexibility can then be obtained by invoking Castigliano's theorem as:

$$c_{ij} = \frac{\partial U_T}{\partial F_i \partial F_j} = \frac{\partial U_0}{\partial F_i \partial F_j} + \frac{\partial U_c}{\partial F_i \partial F_j} \tag{5a}$$

$$\text{or} \qquad c_{ij} = c_{ij,0} + c_{ij,c} \tag{5b}$$

where, c_{ij} is the total local flexibility and F_i is the force applied on the i^{th} DOF of the beam node. $c_{ij,0}$ is the flexibility of the intact beam element, and $c_{ij,c}$ is the additional flexibility due to the presence of the crack.

The details of the flexibility matrix have been well documented [25-27]. The flexibility matrix can be easily converted to a stiffness matrix for the cracked beam element through matrix inversion and a

transformation matrix $\boldsymbol{T}$. This approach was used by the original authors in the analysis of the vibration of cracked beams and the investigation of the effect of coupling between transverse and torsional or longitudinal vibrations [26, 27].

The same general approach via the additional flexibility due to a crack has been employed by several other authors to derive the cracked beam element for the beam vibration analysis or detection of a crack. Qian, et al. [29] developed FE model with the cracked beam element to study the dynamic behaviour of a beam with crack closure. Lee and Chung [30] incorporated the cracked beam element in a procedure involving the rank-ordering technique to detect a crack with just the first four natural frequencies. However, the proposed procedure was limited to a single crack in a beam. Moreover, the effect of axial force was not considered. Zheng and Kessissoglou [31] looked upon the cracked beam element with an arbitrary crack location, and examined the effect of the relative location of the crack on the additional flexibility of the beam element and hence the free vibration properties of the beam. Darpe, et al. [32] studied the effect of coupling between bending, longitudinal and torsional vibrations of a circular shaft using the cracked beam element approach. The cracked segment was modelled using the cracked beam element while the remaining beam was modelled using the intact beam element model. Modelling of the □breathing□behaviour of a crack during the rotor operation was also investigated. Nahvi and Jabbari [33] employed the cracked beam element model in a flexural condition, without considering the axial DOFs, in a finite element analysis to generate the natural frequencies and mode shapes for a beam with a single crack. The FE results are used in a match-up procedure to identify the location and depth of the crack in an experimental beam.

In summary, it seems fair to state that the cracked beam element model formulated on the basis of the additional flexibility has overall superiority comparing to the other approaches. Using this model, the effects of a crack on the various aspects of the beam vibration, including coupling among the transverse, torsional and longitudinal vibrations, have been studied. The utilisation of the model for the detection of cracks in a beam has also been explored but this has largely been limited at a very basic level, and mostly with consideration of just a single crack. There is still a considerable scope to develop a more comprehensive approach to extend the use of this basic model to more complete identification of crack damages in a beam. Factors such as the randomness of the crack location, crack depth and the possible presence of multiple cracks should ideally all be taken into account.

3 Cracked beam element model for crack identification: model formulation and forward verification

The cracked beam element model based on local flexibility and fracture mechanics is adopted here for

the identification of cracks in thick beams. For the sake of completeness, the essential model formulation is described first. The model is then verified for the calculation of the natural frequencies and mode shapes of cracked thick beams in order to check the robustness of the model for both lower and higher modes. The reduced stiffness model is used for the current model to compare with throughout the verification.

As a matter of clarity, herein we define "thick" beams as those having a length to sectional thickness (depth) ratio in the range of 5 to 15. Such beams represent the majority of beams in civil engineering structures. As has been stated, the shear deformation and rotational inertia will have marked influence on the vibration of thick beams. Therefore the formulation of the cracked beam element is based on the Timoshenko beam theory. For the present study, a plane-stress beam with a rectangular section is considered. The same general approach and basic observations will apply for beams with other section geometry, but specific local flexibility (and hence stiffness) needs to be derived accordingly.

3.1 Model formulation

A cracked beam element with the full 6 DOFs in the two-dimensional space is shown in Fig. 5. The crack is located at a distance of l_c from the left node and the crack depth is a. We define the ratio of crack depth a to the sectional depth h as the crack depth ratio α, $\alpha = a/h$. The width of the beam element is b.

It is well known that for relatively thick beams, the shear deformation and rotational inertia of the beams cannot be ignored. For cracked thick beams, the problem still exists. Several authors have observed the difference in the vibrational properties between Euler and Timoshenko models for cracked beams (Kikidis and Papadopoulos [34]; Lele and Maiti [22]; Swamidas, et al. [35]; Aydin [36]). The general conclusion is that the relative difference between the modal data estimated from the two models varies with the crack depth. To eliminate such modelling errors we have used Timoshenko beam model for the cracked element here.

Besides, the axial DOFs are considered in the cracked beam element formulation. It will be shown in the next section (3.2) that there will be coupling terms between the longitudinal and transverse or rotational DOFs in the stiffness matrix for the cracked element. The effect on the free vibration of the cracked beam is that coupling modes of longitudinal and transverse motions will appear, as has been extensively studied for shaft and rotor members (Papadopoulos and Dimarogonas [26] and [27]; Darpe, et al. [32]). The coupling effect is stronger for thicker beams, as demonstrated by Kikidis and Papadopoulos [34], and thus it is considered in the current model.

The flexibility of the cracked element can be established using the energy approach in conjunction with the fracture mechanics principle, as has been summarized in Section 2.3. As shown in Eq. (3),

the strain energy in the cracked beam element under a generalised load is equal to the strain energy of the intact beam element plus the additional strain energy brought by the crack. The additional strain energy due to the presence of crack can be evaluated by the fracture energy. Let the 3 DOFs at the left node be fixed, and the generalised load be axial load P (u_2), shear force Q (v_2) and bending moment M (θ_2).

According to fracture mechanics, the additional strain energy brought by the crack U_c for the beam element in Fig. 5 can be expressed as:

$$U_c = b\int_0^a G\mathrm{d}a \tag{6}$$

The relationships between the energy release rate G and the SIFs are shown in Eq. (4). For the cracked element considered here, only the first two types of SIFs exist. Relationships between the SIFs and the applied loads are shown in Eq. (7) from the standard fracture mechanics theory:

$$K_{\mathrm{I1}} = \frac{P}{bh}\sqrt{\pi a}F_{\mathrm{I1}}(\alpha) \tag{7a}$$

$$K_{\mathrm{I2}} = \frac{6M}{bh^2}\sqrt{\pi a}F_{\mathrm{I2}}(\alpha) \tag{7b}$$

$$K_{\mathrm{II}} = \frac{Q}{bh}\sqrt{\pi a}F_{\mathrm{II}}(\alpha) \tag{7c}$$

where K_{I1} and K_{I2} takes into account the stress brought by axial force and moment, respectively, and K_{II} takes into account the stress brought by the shear force. $F_{\mathrm{I1}}(\alpha)$, F_{I2} (α) and $F_{\mathrm{II}}(\alpha)$ are dimensionless terms and they are expressed as (Tada, et al. [28]):

$$F_{\mathrm{I1}}(\alpha) = \sqrt{\frac{2}{\pi\alpha}\tan\frac{\pi\alpha}{2}}\cdot\frac{0.752+2.02\alpha+0.37(1-\sin 0.5\pi\alpha)^3}{\cos 0.5\pi\alpha} \tag{8a}$$

$$F_{\mathrm{I2}}(\alpha) = \sqrt{\frac{2}{\pi\alpha}\tan\frac{\pi\alpha}{2}}\cdot\frac{0.923+0.199(1-\sin 0.5\pi\alpha)^4}{\cos 0.5\pi\alpha} \tag{8b}$$

$$F_{\mathrm{II}}(\alpha) = \frac{1.122-0.561\alpha+0.085\alpha^2+0.180\alpha^3}{\sqrt{1-\alpha}} \tag{8c}$$

For current loading case with axial force P, shear force Q and bending moment M, the strain energy release rate G can be written as (Tada, et al. [28]):

$$G = \frac{1}{E'}\left(\frac{P}{bh}\sqrt{\pi a}F_{\mathrm{I}1}(\alpha)+\frac{6(M+Ql_e-Ql_c)}{bh^2}\sqrt{\pi a}F_{\mathrm{I}2}(\alpha)\right)^2+\left(\frac{Q}{bh}\sqrt{\pi a}F_{\mathrm{II}}(\alpha)\right)^2 \tag{9}$$

On the other hand, the strain energy of an intact Timoshenko beam element U_0 can be calculated as:

$$U_0 = \frac{1}{2}\int_0^{l_e}\left(\frac{(M+Ql_e-Qx)^2}{EI}+\frac{Q^2}{GA_e}+\frac{P^2}{EA}\right)dx \tag{10}$$

where, A_e is the effective shear area of the beam section and for rectangular section, A_e=5/6A.

With Eq. (5), (9) and (10), the additional and intact flexibility for the cracked beam element can be calculated respectively as:

$$c_{ij,c} = \frac{\partial^2}{\partial F_i \partial F_j}\int_0^a \frac{b}{E'}\left(\frac{P}{bh}\sqrt{\pi a}F_{\mathrm{I}1}(\alpha)+\frac{6(M+Ql_e-Ql_c)}{bh^2}\sqrt{\pi a}F_{\mathrm{I}2}(\alpha)\right)^2+\left(\frac{Q}{bh}\sqrt{\pi a}F_{\mathrm{II}}(\alpha)\right)^2 da \tag{11a}$$

$$c_{ij,0} = \frac{\partial^2}{\partial F_i \partial F_j}\frac{1}{2}\int_0^{l_e}\left(\frac{(M+Ql_e-Qx)^2}{EI}+\frac{Q^2}{GA_e}+\frac{P^2}{EA}\right)dx \tag{11b}$$

where, i, j = 1, 2, 3, and F_1=P, F_2=Q, F_3=M.

It can be seen that there are 2 parameters representing the crack information in c_{ij}, as crack depth a and crack location l_c.

The complete 6×6 stiffness matrix for the element can be obtained by inverting the flexibility matrix and satisfying the force equilibrium in the elements, as follows:

$$K_c = T * C^{-1} * T^T \tag{12}$$

where $\boldsymbol{C}$ is the 3×3 flexibility matrix with c_{ij} as its elements. $\boldsymbol{T}$ is the transforming matrix,

$$T = \begin{bmatrix} -1 & 0 & 0 \\ 0 & -1 & 0 \\ 0 & -l_e & -1 \\ 1 & 0 & 0 \\ 0 & 1 & 0 \\ 0 & 0 & 1 \end{bmatrix} \tag{13}$$

3.2 Discussion on the cracked beam stiffness matrix

For any relative location and depth of the crack, the additional and intact flexibility terms can be evaluated from Eq. (11), and subsequently the stiffness matrix can be calculated according to Eq. (12). In a standard form, $\boldsymbol{K}_c$ can be written as:

$$K_c = \begin{bmatrix} k_{11} & k_{12} & k_{13} & k_{14} & k_{15} & k_{16} \\ & k_{22} & k_{23} & k_{24} & k_{25} & k_{26} \\ & & k_{33} & k_{34} & k_{35} & k_{36} \\ & & & k_{44} & k_{45} & k_{46} \\ & sym & & & k_{55} & k_{56} \\ & & & & & k_{66} \end{bmatrix} \tag{14}$$

The stiffness terms in the matrix can be subdivided into two groups; the diagonal elements k_{ii} (i=1, 2, □ ,6), which represent the driving stiffness of the 6 DOFs, and the off-diagonal elements k_{ij} (i, j=1, 2, □ ,6, and i□j), which represent the coupling between two different DOFs. It should be noticed that the elements in the stiffness matrix are not all independent. Due to the force equilibrium relationship, some elements are the linear combination of others. For example, there are relationships as $k_{12} = -k_{24} = -k_{15} = k_{45}$, and $k_{26} = k_{22}*l_e - k_{23}$.

To illustrate the influence of the crack parameters on the elements of the matrix, it is convenient to use a numerical example. We use a beam element with l_e = 100 mm, h = 100 mm, b = 50 mm and the material properties are set as E = 2.01 GPa, ν = 0.3 and ρ = 7850 kg/m^3. A crack is set at a distance l_c from the left node, with a depth ratio $\alpha = a/h$. The ranges of the two crack parameters are set as: α = 0-0.5, and l_c = 0-50 mm.

Firstly the influence of the crack depth ratio is examined. Let the crack location be fixed at l_c = 25 mm and the crack depth ratio α varies in the above mentioned range to observe the trend of the matrix elements. For those stiffness elements which have the same absolute value, only the common absolute value is presented.

To demonstrate the crack effect we define a ratio β_{ij} in Eq. (15), where k_{ij} (α = 0) is the value of the stiffness element for the intact beam element. It should be noted that some off-diagonal elements such as k_{12}, k_{13} and k_{16} have zero values for the intact beam, and for these elements a reference value at α = 0.05 is used as the respective denominator in the calculation of β_{ij}.

$$\beta_{ij} = \frac{k_{ij}(\alpha)}{k_{ij}(\alpha = 0)} \tag{15}$$

The β_{ij} versus α relationships are presented in Fig. 6. The diagonal elements of the stiffness matrix are shown in Fig. 6(a), and it can be seen that in general these stiffness values reduce markedly with the

increase of the crack depth ratio. The reduction of the diagonal elements is quite natural and it is in line with the stiffness reduction due to the crack. It is worth noting, however, that different DOFs show different rate of stiffness reduction. In the current example, element k_{33} (rotational stiffness) has the largest sensitivity to α; for $\alpha = 0.3$, the ratio of k_{33} is about 0.6 as compared to k_{22} (translational stiffness) of about 0.85.

For the off-diagonal elements, it can be seen from Fig. 6(b) that element k_{26}, which represents the transfer stiffness between the translational DOF of the left node and the rotational DOF of the right node, has a slight increase instead of decrease when α is in the range of 0-0.35. This is because from equilibrium k_{26} can be calculated as $k_{22}*l_e - k_{23}$. When the reduction rate of $k_{22}*l_e$ is smaller than that of k_{23}, k_{26} will increase as appears in Fig. 6(b).

The off-diagonal elements that represent the transfer stiffness between the longitudinal and translational or rotational DOFs, such as k_{12}, k_{13} and k_{16}, are shown in Fig. 6(c). It should be noted that these elements are all zero in the matrix for the intact beam. But they are no longer zero when an asymmetric (single-edge) crack is present which brings eccentricity to the cracked section. The absolute values of these elements increase persistently with increase of the crack depth. The result of these off-diagonal elements being non-zero is that coupling between the longitudinal and translational modes will appear in the structural vibration.

To observe the influence of crack location l_c on the stiffness matrix elements, the crack depth ratio α is fixed as 0.5 and the crack is gradually moved from the left node to the middle of the beam element. A location influence ratio γ_{ij} is defined with respect to the stiffness when the crack is located at the left end of the beam element as:

$$\gamma_{ij} = \frac{k_{ij}(l_c)}{k_{ij}(\alpha = 0.5, l_c = 0)} \tag{16}$$

Fig. 7 illustrates the γ_{ij} versus l_c relationships. Different trends are observed for the different stiffness elements. Take the diagonal elements for example, k_{22} and k_{33} increase with l_c while k_{11} and k_{66} show the opposite trend.

The above analysis shows that the changes of the matrix elements in relation to the changes of the crack parameters differ significantly from what may be represented by assuming a uniform change of the element stiffness as adopted in the reduced stiffness model. Some stiffness elements will decrease to a varying extent with the increase of crack parameters, while some other elements will increase. The transfer stiffness elements relating the axial and translational or rotational DOFs, which are zero in the intact beam matrix, will no longer be zero in the cracked beam element. These actual effects of the crack parameters on the beam stiffness matrix illustrate from a mathematic point of view why the

reduced stiffness model cannot accurately predict the modal parameters of the example cracked beam shown in Section 1.

3.3 Forward verification of the cracked beam model for the dynamic properties

The performance of the cracked beam element described in Section 3.1 in the analysis of the beam vibration, herein concerning particularly the modal frequencies and mode shapes, is verified with numerical examples, in which refined continuum finite element models are employed to simulate the actual cracked beams and generate the required model data. Using such refined FE models essentially creates the "exact" modal data while avoids other complications such as noises, thus allowing the verification of the performance of the cracked beam element model in comparison with other beam element models at a fundamental level. A beam with the following properties is simulated: $L \times b \times h$ = 1000×50×100 mm. Material properties are set as: E = 201 GPa, ν = 0.3, ρ = 7850 kg/m^3.

The crack is set at L_c = 350 mm from the left support of the beam. Two crack depth ratios, α = 0.3 and 0.5, are used in the calculations. It should be noted at this juncture that the crack problem concerned in this paper is related to damage identification applications, and so the basic scenario is associated with generally loaded (e.g. by gravity) structures. As such the crack is presumed to remain in an open state during small vibration tests from which the modal properties are extracted. Therefore, the crack gap closing issue is not under consideration.

Several representative boundary conditions, namely free-free, simply supported (with a span as 1000 mm), and fixed-free (cantilever), are considered in the verification, as shown in Fig. 8. For the verification within this paper, we shall use refined continuum finite element model with solid elements to produce the benchmark data for the comparison of the results from the cracked beam element model. Using refined FE model with solid elements can represent sufficiently well the spatial effect of the cracks on the beam behaviour, and at the same time does not involve complications from sources such as measurement errors and other imperfection from physical tests, and therefore serves exactly the purpose of examining the soundness of the cracked beam element model. In the subsequent descriptions, the term "measured" data will refer to the simulated data from the numerical experiments using the refined finite element model unless specified otherwise.

To accurately model the effect of the crack, the mesh density is increased towards the crack tip, as depicted in Fig. 9.

In the parallel model using beam elements, 10 Timoshenko beam elements, including 9 intact and 1 cracked, are used. Timoshenko stiffness and mass matrices with high-accuracy cubic shape functions are used for the intact elements, while the cracked beam element model described in Section 3.1 is used for the cracked element. Both longitudinal and transverse modes are calculated with the FE

model but only the transverse modes are discussed below. The reason is that longitudinal modes are less frequently used in damage identification due to the difficulties of measuring them in real-life structures. To verify the accuracy of the cracked beam element model, two indicators are used in the comparison. The first one is the shift of the natural frequency brought by the crack, S_i,

$$S_i = \frac{f_i^0 - f_i^{\mathrm{d}}}{f_i^0} \times 100\% \tag{17}$$

where f_i^0 and f_i^{d} are the i^{th} natural frequencies of the intact and cracked beams, respectively. By normalising the modal data to the respective reference model, the modelling errors such as that due to discretisation can be largely neutralised in the comparisons. The "measured" and predicted natural frequency shifts will be compared.

The second indicator is the Modal Assurance Criterion (MAC), which measures the consistency of two mode shapes,

$$\mathrm{MAC}_i = \frac{\left| \left\{\phi_i^{\mathrm{m}}\right\}^T \left\{\phi_i^{\mathrm{c}}\right\} \right|^2}{\left| \left\{\phi_i^{\mathrm{m}}\right\}^T \left\{\phi_i^{\mathrm{m}}\right\} \right| \cdot \left| \left\{\phi_i^{\mathrm{c}}\right\}^T \left\{\phi_i^{\mathrm{c}}\right\} \right|} \tag{18}$$

where, $\left\{\phi_i^{\mathrm{m}}\right\}$ and $\left\{\phi_i^{\mathrm{c}}\right\}$ are the "measured" and predicted i^{th} mode shapes of the cracked beam, respectively.

The reduced stiffness method is also used in a separate beam model to facilitate a cross-comparison with the cracked beam element model. To obtain an "equivalent" reduced elemental stiffness ratio, D_e, for a given crack scenario, the first five natural frequencies are used in an updating process to come up with a best estimate of the D_e value.

Frequency shifts of the first 6 modes are compared in Fig. 10 and 11. It can be seen that the "measured" and predicted results using the cracked beam element model match quite well for all modes. In contrast, the reduced stiffness model can only predict the frequency shifts consistently for the first two modes, and large errors occur in the higher modes, and for some modes the percentage error is even larger that the frequency shift itself. This echoes the discussions in Section 1 and Section 3.2.

The MAC results for the first 6 mode shapes are compared. The results for both crack cases are similar and so only the comparison for $\alpha = 0.5$ is shown here, Fig. 12. It can be seen that the MAC values with the crack model are all greater than 0.99, indicating very good match between the "measured" and predicted mode shapes. The reduced stiffness model is also able to get quite satisfactory MAC values for lower modes; however, the results are not so good for higher modes.

The comparisons show that the cracked beam element model is able to predict the natural frequencies as well as the mode shapes of the cracked beam for a sufficient number of 6 modes with very good accuracy. The reduced stiffness method, in contract, can only produce satisfactory results for the lowest 2-3 modes, and errors in the higher modes are significant.

4 Crack damage identification using the cracked beam element model

In this section the cracked beam element model will be implemented in a finite element model updating framework for the identification of crack damage in structural beams.

4.1 General considerations

In this approach, the beam in question is discretized into a suitable number of beam elements. The following rules should be taken into consideration when deciding the mesh size: a) the model should be sufficiently accurate in representing the vibration properties of the beam while at the same time keep the updating parameters as few as possible, b) it should facilitate representation of single crack or multiple cracks across the length of the beam; in this respect it should be consistent with the cracked beam element formulation with consideration of the influence range of a crack.

Considering that the influence range of a major crack would be the order of the beam depth, it is reasonable to adopt a discretization with individual element length l_e equal or around the sectional depth. As demonstrated in previous sections, a Timoshenko beam model with this level of discretization while using the cubic-shape function will be sufficiently accurate for at least the first 6 modes, which should well cover the actual measurable number of modes in structural beams in practice.

For model updating purpose, each beam element is assumed to be a possible cracked element and hence is modelled with the pair of variable crack parameters (α_i , l_{ci}), namely the crack depth ratio and the relative location within element i.

It can be seen that the total number of variable parameters to be updated when using the cracked beam element model is twice the number of beam elements in the model, or twice the number of variable parameters when using the reduced stiffness model. But as both the location and depth of the crack can be updated from the cracked beam model, and to achieve a similar updating effect many times more refined discretisation would have to be employed in a reduced stiffness approach, the updating demand with the cracked beam model is in effect considerably reduced.

4.2 Adaptive discretization

Another important aspect that needs to be handled appropriately is the possible conflict between the beam discretisation and the physical influence range of a crack, in a situation where a crack is too close to one end of an individual element, making the effect of such a crack to "spill over" to the adjacent element. To illustrate the situation, we only need to use a conceptual analysis. Assume that the influence range of the crack is symmetric to the crack (which is not necessarily true in real structures) and that the crack influence range is contained within an individual element length. If the mesh of the beam model is made in such a way that the crack is around the centre of a cracked element, we can be generally satisfied that the influence of an individual crack is covered within a single element, as shown in Fig. 13(a). Thus, the crack depth and exact location could be identified in a more straightforward manner from the model updating. However, if the crack is close to the left or right node of the element, the influence range of the crack is likely to cross into the immediate adjacent element, as depicted in Fig. 13(b) and (c). The implication on the inverse calculation (model updating) is that two cracks might be identified in the two adjacent elements, which would not be correct. More detailed examples will be given in the next section.

To tackle the above potential problem, an adaptive process is proposed herein. In this process, an adapted discretization will be involved if the first identification turns out to indicate two cracks which are too closely spaced within two adjacent elements. As a general guide, we propose to use a distance of $0.5h$ as a limiting criterion. In such a situation, the model will be re-meshed such that the influence range of the real crack can be mostly covered in one element, and the updating procedure is repeated on the adapted mesh.

Assuming that two closely spaced cracks satisfying the above distance threshold occur in the initial updating results, in element p-1 (crack depth ratio $\alpha_{p\text{-}1}$) and element p (crack depth ratio α_p). The real crack should lie between the two identified cracks, and the real crack location (L_c) may be estimated using a simple interpolation method as:

$$L_c' = \frac{\alpha_{p-1} L_{c,p-1} + \alpha_p L_{c,p}}{\alpha_{p-1} + \alpha_p} \tag{19}$$

where $L_{c,p\text{-}1}$ and $L_{c,p}$ denote the locations of the two closely spaced cracks detected from the initial updating.

The adapted mesh will set the above estimated crack location to around the centre of the cracked element. The detailed process and the effectiveness of this adaptive approach will be illustrated in the examples in the Section 4.4.

4.3 Parameter updating algorithm

Genetic algorithm (GA) is employed to perform the FE model updating for the cracked beam. GA has

been used as an optimisation tool in civil engineering in the last several decades (Perera and Torres [37]). Compared with traditional methods, GA-based model updating has several advantages. For example, the GA searching results do not depend on the initial setting of the updating parameters, thus a global optimal result, rather than local, is generally guaranteed. This makes the updating search more robust. There is also no need to calculate the sensitivity matrix of the structure during the updating process. There have been many successful applications using GA in model updating problems (e.g. Perera and Torres [37]; Tu and Lu [38]).

Various objective functions have been employed for model updating in the literature (Friswell, et al. [39]; Teughels, et al. [40]; Hao and Xia [41]). A general form of the objective function incorporating both eigenvalue and mode shape data is shown in Eq. (20),

$$J = \frac{1}{N_{\mathrm{f}}} \sum_{i=1}^{N_{\mathrm{f}}} W_i \cdot \mathrm{abs}\left(\frac{\lambda_{\mathrm{m}i}^{\mathrm{d}}}{\lambda_{\mathrm{m}i}^{0}} - \frac{\lambda_{\mathrm{c}i}^{\mathrm{d}}}{\lambda_{\mathrm{c}i}^{0}} \right) + \frac{1}{N_{\mathrm{s}} N_{\mathrm{n}}} \sum_{i=1}^{N_{\mathrm{s}}} V_i \cdot \left[\sum_{j=1}^{N_{\mathrm{n}}} \mathrm{abs}\left(\varphi_{\mathrm{m}ji}^{\mathrm{d}} - \varphi_{\mathrm{c}ji}^{\mathrm{d}} \right) \right] \tag{20}$$

where, J is the objective function to be minimised, λ denotes the eigenvalue (= $(2\pi f)^2$), φ denotes the mode shape displacement, with the subscript 'm' indicating measured data and 'c' computed data, and the superscript 'd' indicating damaged (current) state and '0' the intact state. N_{f} is the number of eigenvalues to be included, N_{s} is the number of mode shapes to be included, N_{n} is the number of nodes in the mode shapes. W_i and V_i are the weights for the i^{th} eigenvalue and mode shape, respectively. It is noted that by using the eigenvalue ratio relative to the measured or computed intact state, the effect of any gross modelling errors brought by factors other than the crack can be reduced.

4.4 Application examples

The cantilever beam presented in Section 3.3 is used as an example to demonstrate the FE model updating and damage identification process. In fact during the study the same identification procedure has also been applied on beams with other boundary conditions including free-free and simply supported beams, and similar identification results as in the cantilever beam, which will be described in detail below, can be obtained.

Firstly, a single crack case is investigated and the crack is assumed to be at L_{c} = 350 mm from the left end of the beam. Two different crack depth ratios are used, with α being 0.3 and 0.5, respectively.

As mentioned in Section 3.3, the 'measured' data are generated from the numerical experiments with 2D solid elements. Because no measurement errors are involved under this circumstance, for simplicity the weights W_i, V_j in the objective function Eq. (20) are set to be unity.

In the FE model, the beam is discretised into 10 elements, so there are totally 10 pairs of crack parameters to be updated when the cracked beam element model is used. It should be pointed out that

for a cantilever beam the element closest to the free end would be entirely insensitive to the eigenvalue and mode shape data, therefore including the parameters of the free end element in the updating process could cause ill-conditioning and hence false updating result for this element. Such a problem could be resolved by resorting to additional measurement data which would have appropriate sensitivity to the free end element, such as the so-called Artificial Boundary Condition (ABC) frequencies (Tu and Lu [38]). As the present study focuses on the effectiveness of the crack model, we simply exclude the free end element in the updating parameters. So a total of 9 pairs or 18 crack parameters are considered in the cracked beam element model.

For a comparison, two sets of "measurement" data are employed for the updating respectively, one includes the first 3 modes of information, and another includes the first 5 modes.

For the search of the optimal solution, the GA function in Matlab is employed. The parametric settings for GA are given in Table 2.

From monitoring the convergence progress during the searching process, it is found that a limit of maximum generation of 1500 is adequate to achieve satisfactory converging result.

4.4.1 Updating results with the cracked beam element model

The updating results using the cracked beam element model are summarised in Table 3 and 4. The updated crack depth ratios are shown in Fig. 14 and 15. Note again that the exact updating results should be a crack in the 4th element with a crack depth ratio α = 0.3 in one case and α = 0.5 in the other case, and l_c = 50 mm.

It can be seen that the updating results with both sets of the modal data can all find the correct cracked beam element. The updated α and l_c values are also reasonably accurate. The results with 5 modes of information are generally better than those with 3 modes. This is normally expected, but it should also be pointed out that the 3rd mode information has low sensitivity to the crack element in this particular case (as can be seen from Fig. 10(c) and 11(c)). So there are effectively only two modes of information in the case of using the first 3 modes.

4.4.2 Updating results with the reduced stiffness model

The performance of the reduced stiffness model is also checked for benchmarking. Similar to the updating in Section 4.4.1, each finite element is treated as a possible cracked element and the stiffness reduction ratio D_{ei} is used as updating parameter. The updating results of D_e are shown in Fig. 16 and 17. It is noted that the last (10th) element at the free end is not involved in the updating (assumed intact).

It can be seen that the updating results are not correct for both crack scenarios when 3 modes of

information are used. The actual crack (in the 4th element) is missed while there are two false cracks in the 2nd and 5th elements. When 5 modes of information are used, the results appear to be acceptable for beam with α = 0.3, but not for beam with α = 0.5, in which two major false cracks occur. The reason for the poor performance is attributable to the significant modelling error in the reduced stiffness model, as demonstrated in Section 3.3. Another thing to note is that it is difficult to interpret the depth and exact location of the identified crack from the updated D_e value with this model, as there is no explicit physical meaning of the parameter.

4.4.3 Updating with a coarse mesh setting

The updating is also examined with a relatively coarse mesh setting. Five elements with l_e = 200 mm are used in the FE model. With the new mesh setting, the crack should be in the 2nd element with l_c = 150 mm. As the reduced stiffness method becomes even less physically meaningful with a coarse mesh, only the cracked beam element model is employed. The complete updating results are listed in Table 5 and the identified crack depth ratios for the α = 0.5 case are shown in Fig. 18.

It can be seen that good results can still be obtained even when only 5 elements are used in the FE model. It is particularly of interest to note that with the coarse mesh of just 5 elements, the explicit crack parameters can be identified quite accurately with modal data from just the first three modes, and the accuracy from using the first three modes is almost the same as using the first five modes. Comparing to the equivalent stiffness method, where a coarse mesh would imply a loss of resolution and hence become less meaningful, the cracked beam model shows a further layer of advantage.

4.4.4 Updating with adaptive discretisation

In the above examples, the crack is located at 350mm from the fixed end of the cantilever beam, and it is at the centre of the 4th beam element in the beam model. Now we consider some non-centred crack scenarios. Two cantilever beams with different crack locations are used in the calculation. Beam1 has a crack at 310mm from the fixed end while Beam2 has a crack at 390mm from the fixed end, as shown in Fig. 19. All the other parameters are kept to be same as the ones used in Section 4.4.1. We still use 10 Timoshenko beam elements with l_e = 100 mm to update the beam model. Thus, the crack is located in the 4th beam element with l_c = 10 mm and l_c = 90 mm for the two beams, respectively, as depicted in Fig. 19. It can be seen that in Beam1, the crack is very close to the left node of the beam element, while the opposite is true in Beam2. The crack depth ratio is set as α = 0.5 for the two beams.

Model updating is then performed to identify the crack parameters. The results are presented in Fig. 20, and Table 6. It can be seen that correct crack element number can be identified in all of the beams. However, the identified crack depth values are all lower than the actual value, especially for Beam1, in which the identified α value is around 15% lower than the actual value. This is apparently

attributable to the fact that a "false" crack is identified in the immediate next element to the actual crack. For Beam1 (l_c = 10 mm), a "false" crack is identified in the left adjacent element, while for Beam2 (l_c = 90 mm), a "false" crack is identified in the right adjacent element.

As has been explained with Fig. 13, the "false" crack is the result of the influence range of the crack stretching into the adjacent element. This problem may be resolved readily using the adaptive approach as described in Section 4.2. With Eq. (19), the real crack location of the two beams can be estimated as L_e = 305 and 395 mm for Beam1 and Beam2, respectively. The two beams are re-meshed to put the crack around the centre of the cracked beam element. Herein a uniform mesh is still used in the re-meshed model while the number of elements is reduced to adjust the boundaries of the cracked element. It is found that when 8 elements are used in Beam 1, the estimated L_e is quite close to the centre of the 3rd element (312.5 mm). As a result, the new mesh size is set as l_e = 1000/8 = 125 mm. The same method is applied on Beam 2, resulting in a new mesh size as l_e = 1000/9 = 111 mm.

Alternatively, the model may be re-meshed just in the neighbouring area of the crack, thus keeping the remaining mesh unchanged, resulting in a non-uniform mesh setting. Either way should fit the purpose as long as the estimated crack location sits around the centre of the cracked element.

With the new mesh setting, the real crack should be in the 3rd element with l_c = 60 mm for Beam 1 and in the 4th element with l_c = 57 mm for Beam2. The FE models with the adapted mesh setting are updated and the results are presented in Table 7 and 8 and Fig. 21. It can be seen that correct crack parameters can be obtained for all of the examples, which proves that the adaptive updating strategy is a success.

4.4.5 Beam with multiple cracks

As has been stated in Section 4.1, there is no restriction on the number of cracks in the model updating with the cracked beam element model, so it can readily be used in the multiple cracks scenarios, barring any closely spaced adjacent cracks. As an example, the same cantilever beam but with 3 cracks, shown in Fig. 22, is used to demonstrate the updating performance.

Using 10 beam elements in the model, the actual cracks are located in elements 2, 4 and 7, and the crack parameters for the three cracks should be [α, l_c] = [0.4, 50], [0.5, 60], and [0.3, 70], respectively. The first 5 modes of information are used in the objective function and model updating results are presented in Table 9 and Fig. 23. It can be seen that the three cracks can all be identified with good accuracy, showing the ability of the current model to identify multiple cracks.

5 Conclusions

A comprehensive finite element model updating procedure has been developed for crack damage identification in thick beams. An individual crack is described using a cracked beam element model involving explicitly the relative crack location and the crack depth. The cracked beam element stiffness matrix is formulated taking into account the additional flexibility brought by the crack in accordance with the fracture mechanics principles. Shear deformation and coupling between the translational and longitudinal DOFs are all represented in the model. Both forward and FE model updating results have demonstrated superior performance of the cracked beam model as benchmarked against the reduced stiffness model. A few more specific conclusions may also be drawn:

(1) From the forward verifications, the cracked beam model can predict sufficiently accurately the natural frequencies and mode shapes of cracked thick beams up to 9 modes (6 modes were shown in the paper), and in a consistent manner. On the other hand, the reduced stiffness model can only predict the modal data accurately for just the lowest couple of modes.

(2) In conjunction with a global searching technique (using GA herein), high quality model updating results can be obtained in both single crack and multiple cracks scenarios. In comparison, the reduced stiffness model has failed to identify the correct crack location in most of the scenarios.

(3) The issue with the crack influence range crossing into the adjacent beam element in the case where the location of the crack is too close to one end of the cracked element can be readily overcome by a simple adaptive procedure. This involves an adaptation of the initial discretization scheme so that the projected crack location from the first estimate is made at around the centre of a beam element in the adapted mesh. The procedure has been verified to result in satisfactory outcome.

(4) The cracked beam model has demonstrated superior performance in coping with limited amount of modal data, while a reduced number of beam elements are employed. This has been achieved without losing the preciseness of the crack identification in any significant way, thanks to the explicit representation of the crack information in the model.

The performance of the model has been established by benchmarking against refined finite element simulations and parallel comparison with the reduced stiffness method. This paper has not involved experimental aspects such as measurement errors. Although there are no specific aspects to suggest that the present approach may be more susceptible to measurement errors comparing to other model-based techniques, verification of the model in an actual measurement and structural environment is important and this will be dealt with in the subsequent study.

Acknowledgements

The research reported in the paper is partly funded by the Chinese Scholarship Council and the University of Edinburgh through a joint scholarship for the PhD study of the first author.

References

[1] S.W. Doebling, C.R. Farrar, M.B. Prime, D.W. Shevitz, Damage identification and health monitoring of structural and mechanical systems from changes in their vibration characteristics: A literature review, Los Alamos National Lab, NM (United States), 1996.

[2] H. Sohn, C.R. Farrar, F.M. Hemez, D.D. Shunk, D.W. Stinemates, B.R. Nadler, J.J. Czarnecki, A review of structural health monitoring literature: 1996-2001, Los Alamos National Laboratory Los Alamos, NM(United States), 2004.

[3] W. Fan, P.Z. Qiao, Vibration-based damage identification methods: A review and comparative study, Structural Health Monitoring-an International Journal 10(2011) 83-111.

[4] J.E. Mottershead, M.I. Friswell, Model updating in structural dynamics - a survey, Journal of Sound and Vibration 167(1993) 347-375.

[5] J.E. Mottershead, M. Link, M.I. Friswell, The sensitivity method in finite element model updating: A tutorial, Mechanical Systems and Signal Processing 25(2011) 2275-2296.

[6] H.P. Chen, T.S. Maung, Regularised finite element model updating using measured incomplete modal data, Journal of Sound and Vibration 333(2014) 5566-5582.

[7] M.I. Friswell, J.E.T. Penny, Crack modeling for structural health monitoring, Structural Health Monitoring-an International Journal 1(2002) 139-148.

[8] B. Peeters, M. Abdel Wahab, G. De Roeck, J. De Visscher, W.P. De Wilde, J.-M. Ndambi, J. Vantomme, Evaluation of structural damage by dynamic system identification, Proceedings of the 21th International Seminar on Modal Analysis, Katholieke Universiteit Leuven, Belgium, 1996, pp. 1349-1362.

[9] M.N. Cerri, F. Vestroni, Use of frequency change for damage identification in reinforced concrete beams, Journal of Vibration and Control 9(2003) 475-491.

[10] J.F. Unger, A. Teughels, G. De Roeck, System identification and damage detection of a prestressed concrete beam, Journal of Structural Engineering-ASCE 132(2006) 1691-1698.

[11] M. Dilena, A. Morassi, Structural health monitoring of rods based on natural frequency and antiresonant frequency measurements, Structural Health Monitoring-an International Journal 8(2009) 149-173.

[12] J.K. Sinha, M.I. Friswell, S. Edwards, Simplified models for the location of cracks in beam structures using measured vibration data, Journal of Sound and Vibration 251(2002) 13-38.

[13] A.D. Dimarogonas, Vibration of cracked structures: A state of the art review, Engineering Fracture Mechanics 55(1996) 831-857.

[14] S. Christides, A.D.S. Barr, One-dimensional theory of cracked Bernoulli-Euler beams, International Journal of Mechanical Sciences 26(1984) 639-648.

[15] M.H.H. Shen, C. Pierre, Natural modes of Bernoulli-Euler beams with symmetric cracks, Journal of Sound and Vibration 138(1990) 115-134.

[16] M.H.H. Shen, C. Pierre, Free vibrations of beams with a single-edge crack, Journal of Sound and Vibration 170(1994) 237-259.

[17] T.G. Chondros, A.D. Dimarogonas, J. Yao, A continuous cracked beam vibration theory, Journal of Sound and Vibration 215(1998) 17-34.

[18] S.H.S. Carneiro, D.J. Inman, Continuous model for the transverse vibration of cracked Timoshenko beams, Journal of Vibration and Acoustics 124(2002) 310-320.

[19] H. Liebowitz, H. Vanderveldt, D. Harris, Carrying capacity of notched columns, International Journal of Solids and Structures 3(1967) 489-500.

[20] H. Okamura, K. Watanabe, T. Takano, Applications of the compliance concept in fracture mechanics, ASTM Special Technical Publication 536(1973) 423-438.

[21] W.M. Ostachowicz, M. Krawczuk, Analysis of the effect of cracks on the natural frequencies

of a cantilever beam, Journal of Sound and Vibration 150(1991) 191-201.
[22] S.P. Lele, S.K. Maiti, Modelling of transverse vibration of short beams for crack detection and measurement of crack extension, Journal of Sound and Vibration 257(2002) 559-583.
[23] E. Viola, L. Nobile, L. Federici, Formulation of cracked beam element for structural analysis, Journal of Engineering Mechanics-ASCE 128(2002) 220-230.
[24] M. Mehrjoo, N. Khaji, M. Ghafory-Ashtiany, New Timoshenko-cracked beam element and crack detection in beam-like structures using genetic algorithm, Inverse Problems in Science and Engineering 22(2014) 359-382.
[25] A.D. Dimarogonas, C.A. Papadopoulos, Vibration of cracked shafts in bending, Journal of Sound and Vibration 91(1983) 583-593.
[26] C.A. Papadopoulos, A.D. Dimarogonas, Coupling of bending and torsional vibration of a cracked Timoshenko shaft, Ingenieur Archiv 57(1987) 257-266.
[27] C.A. Papadopoulos, A.D. Dimarogonas, Coupled longitudinal and bending vibrations of a rotating shaft with an open crack, Journal of Sound and Vibration 117(1987) 81-93.
[28] H. Tada, P.C. Paris, G.R. Irwin, The stress analysis of cracks handbook, The American Society of Mechanical Engineers, New York, 2000.
[29] G.L. Qian, S.N. Gu, J.S. Jiang, The dynamic behavior and crack detection of a beam with a crack, Journal of Sound and Vibration 138(1990) 233-243.
[30] Y.S. Lee, M.J. Chung, A study on crack detection using eigenfrequency test data, Computers & Structures 77(2000) 327-342.
[31] D.Y. Zheng, N.J. Kessissoglou, Free vibration analysis of a cracked beam by finite element method, Journal of Sound and Vibration 273(2004) 457-475.
[32] A.K.Darpe, K. Gupta, A. Chawla, Coupled bending, longitudinal and torsional vibrations of a cracked rotor, Journal of Sound and Vibration 269(2004) 33-60.
[33] H. Nahvi, M. Jabbari, Crack detection in beams using experimental modal data and finite element model, International Journal of Mechanical Sciences 47(2005) 1477-1497.
[34] M.L. Kikidis, C.A. Papadopoulos, Slenderness ratio effect on cracked beam, Journal of Sound and Vibration 155(1992) 1-11.
[35] A.S.J. Swamidas, X. Yang, R. Seshadri, Identification of cracking in beam structures using Timoshenko and Euler formulations, Journal of Engineering Mechanics-ASCE 130(2004) 1297-1308.
[36] K. Aydin, Influence of crack and slenderness ratio on the eigenfrequencies of Euler-Bernoulli and Timoshenko beams, Mechanics of Advanced Materials and Structures 20(2013) 339-352.
[37] R. Perera, R. Torres, Structural damage detection via modal data with genetic algorithms, Journal of Structural Engineering-ASCE 132(2006) 1491-1501.
[38] Z.G. Tu, Y. Lu, FE model updating using artificial boundary conditions with genetic algorithms, Computers & Structures 86(2008) 714-727.
[39] M.I. Friswell, J.E. Mottershead, H. Ahmadian, Combining subset selection and parameter constraints in model updating, Journal of Vibration and Acoustics 120(1998) 854-859.
[40] A. Teughels, J. Maeck, G. De Roeck, Damage assessment by FE model updating using damage functions, Computers & Structures 80(2002) 1869-1879.
[41] H. Hao, Y. Xia, Vibration-based damage detection of structures by genetic algorithm, Journal of Computing in Civil Engineering 16(2002) 222-229.

Table 1 Identified D_e values from different modes

Mode	D_e
1	0.653
2	0.636
3	0.119
4	0.111
5	0.668
6	0.491
Mean	0.446
Standard deviation/mean	0.592

Table 2 Parametric settings for GA

Parameter	Setting
Population size	5000
Fitness limit	-Infinite
Max generation	1500
Crossover fraction	0.7
Mutation rate	0.02

Table 3 Updating results of cantilever beam with $\alpha = 0.3$

Element number	1	2	3	**4**	5	6	7	8	9	10
l_c/mm (3 modes)	100.0	90.5	83.9	**60.2**	0.0	0.0	15.6	99.6	100.0	0.0
l_c/mm (5 modes)	100.0	16.1	100.0	**50.3**	0.0	78.2	0.0	40.9	100.0	0.0

Table 4 Updating results of cantilever beam with $\alpha = 0.5$

Element number	1	2	3	**4**	5	6	7	8	9	10
l_c/mm (3 modes)	98.3	91.6	94.3	**43.7**	0.0	0.0	0.2	95.4	100.0	0.0
l_c/mm (5 modes)	100.0	29.9	99.3	**50.3**	0.0	57.8	0.0	89.3	100.0	0.0

Table 5 Updating results of cantilever beam with 5 elements

Crack depth ratio	$\alpha = 0.3$					$\alpha = 0.5$				
Element number	1	**2**	3	4	5	1	**2**	3	4	5
l_c/mm (3 modes)	179.3	**146.6**	10.7	45.1	174.2	174.2	**150.6**	0.2	157.1	0.0
l_c/mm (5 modes)	165.2	**164.1**	0.0	0.0	181.5	181.5	**152.6**	44.7	7.2	0.0

Table 6 Updating results of cantilever beams with non-centred crack

Element number	1	2	3	**4**	5	6	7	8	9	10
l_c/mm (Beam1)	75.1	0.0	99.9	**9.5**	26.2	44.9	42.2	12.5	100.0	0.0
l_c/mm (Beam2)	0.1	0.0	100.0	**85.7**	29.9	0.1	46.0	0.0	100.0	0.0

Table 7 Updating results with adapted mesh (Beam1)

Element number	1	2	**3**	4	5	6	7	8
l_c/mm	115.5	33.5	**56.1**	75.9	28.8	83.7	124.0	0.0

Table 8 Updating results with adapted mesh (Beam2)

Element number	1	2	3	**4**	5	6	7	8	9
l_c/mm	111.0	40.8	0.1	**59.1**	99.1	58.9	0.2	111.1	0.0

Table 9 Updating results of beam with multiple cracks

Element number	1	**2**	3	**4**	5	6	**7**	8	9	10
l_c/mm	100.0	**55.2**	0.0	**59.7**	0.0	29.7	**64.0**	87.4	100.0	0.0

Figure captions

Fig. 1 Example beams with a length to sectional depth ratio of 10 (Unit: mm). (a) Intact; (b) Cracked

Fig. 2 Measured and predicted frequency shifts

Fig. 3 Stiffness reduction of cracked element. (a) Cracked beam segment; (b) Stiffness distribution.

Fig. 4 Discrete spring model. (a) Cracked beam segment; (b) Cracked beam model.

Fig. 5 Loading state of a cracked beam element

Fig. 6 Influence of crack depth ratio on the elements of stiffness matrix. (a) Diagonal elements; (b) Off-diagonal elements relating translational and rotational DOFs; (c) Off-diagonal elements relating longitudinal and translational or rotational DOFs.

Fig. 7 Influence of crack location on the elements of stiffness matrix. (a) Diagonal elements; (b) Off-diagonal elements relating translational and rotational DOFs; (c) Off-diagonal elements relating longitudinal and translational or rotational DOFs.

Fig. 8 Boundary conditions of the beams. (a) Free-free; (b) Simply supported; (c) Cantilever.

Fig. 9 Mesh of the FE model with solid elements

Fig. 10 Comparisons between measured and predicted frequency shifts (α = 0.3). (a) Free-free beam; (b) Simply supported beam; (c) Cantilever beam.

Fig. 11 Comparisons between measured and predicted frequency shifts (α = 0.5). (a) Free-free beam; (b) Simply supported beam; (c) Cantilever beam.

Fig. 12 Comparison between MAC results from two different models (α = 0.5). (a) Free-free beam; (b) Simply supported beam; (c) Cantilever beam.

Fig. 13 Relationship between the crack influence range and the beam element. (a) Crack at element centre; (b) Crack close to left node; (c) Crack close to right node.

Fig. 14 Updating results of cantilever beam with α = 0.3. (a) With 3 modes; (b) With 5 modes.

Fig. 15 Updating results of cantilever beam with α = 0.5. (a) With 3 modes; (b) With 5 modes.

Fig. 16 Updating results of cantilever beam with α = 0.3. (a) With 3 modes; (b) With 5 modes.

Fig. 17 Updating results of cantilever beam with α = 0.5. (a) With 3 modes; (b) With 5 modes.

Fig. 18 Updating results of cantilever beam with $\alpha = 0.5$. (a) With 3 modes; (b) With 5 modes.

Fig. 19 Examples with adaptive updating strategy (Unit: mm). (a) Beam1; (b) Beam2.

Fig. 20 Updating results of beams with non-centred crack. (a) Beam1; (b) Beam2.

Fig. 21 Updating results with adapted mesh. (a) Beam1; (b) Beam2.

Fig. 22 Beam with multiple cracks

Fig. 23 Updating results of beam with multiple cracks

Figure(s)

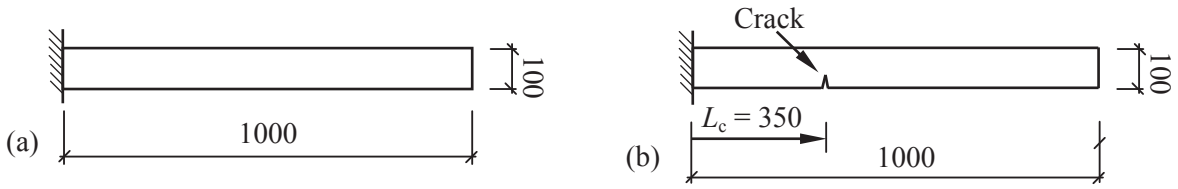

Fig. 1 Example beams with a length to sectional depth ratio of 10 (Unit: mm). (a) Intact; (b) Cracked

Figure(s)

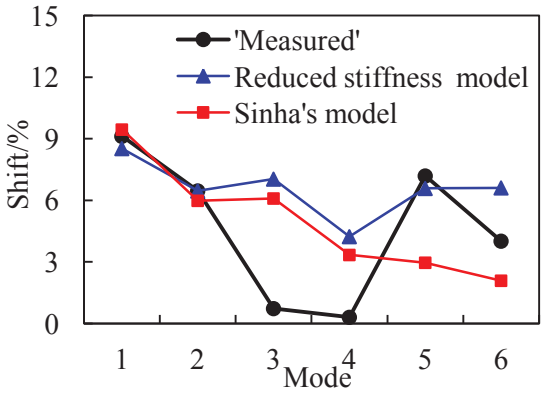

Fig. 2 ‘Measured’ and predicted frequency shifts

Figure(s)

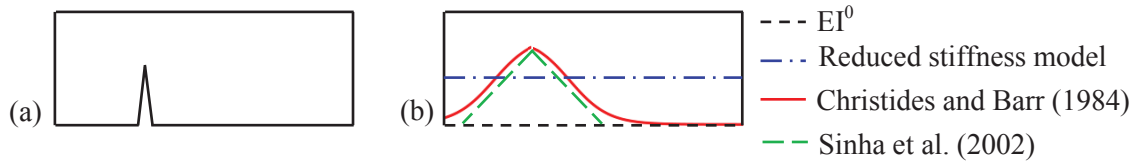

Fig. 3 Stiffness reduction of cracked element. (a) Cracked beam segment; (b) Stiffness distribution.

Figure(s)

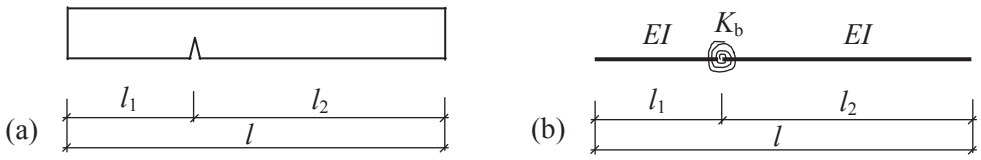

Fig. 4 Discrete spring model. (a) Cracked beam segment; (b) Cracked beam model.

Figure(s)

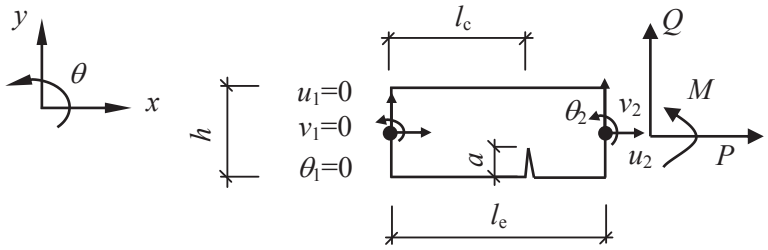

Fig. 5 Loading state of a cracked beam element

Figure(s)

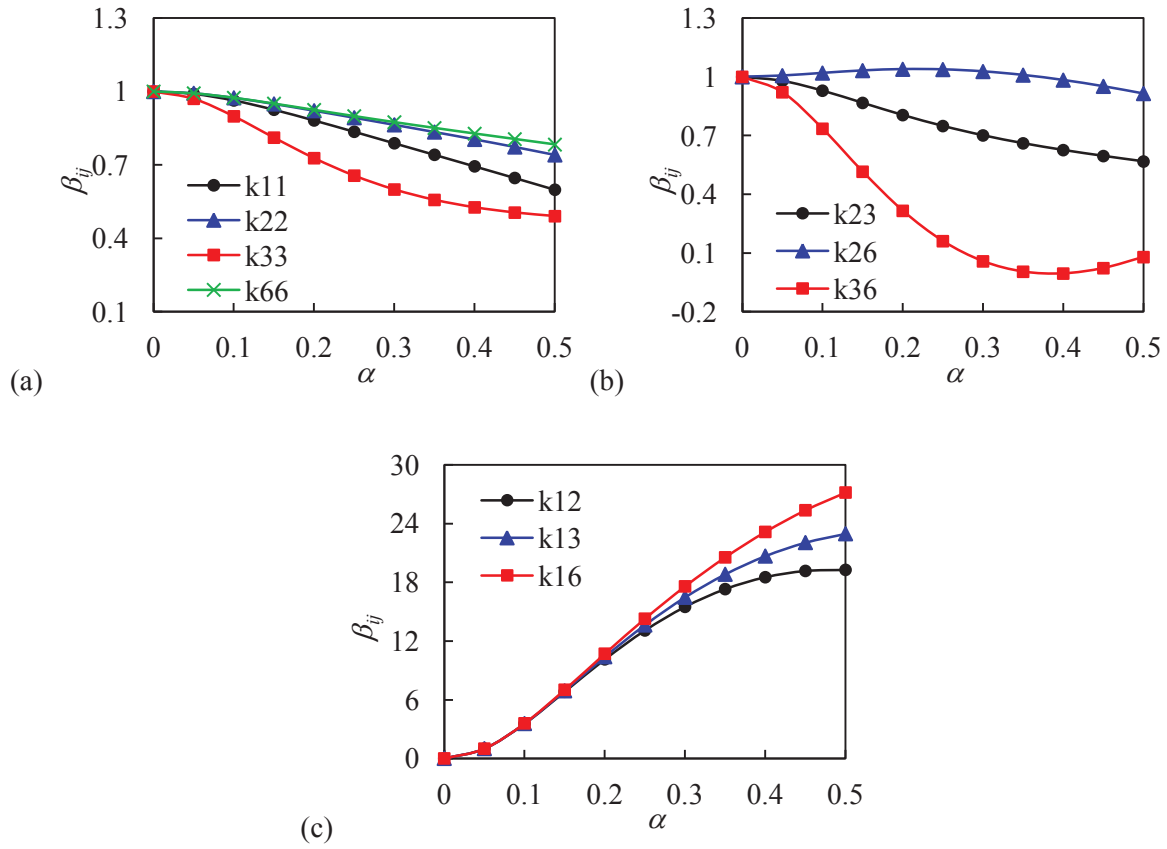

Fig. 6 Influence of crack depth ratio on the elements of stiffness matrix. (a) Diagonal elements; (b) Off-diagonal elements relating translational and rotational DOFs; (c) Off-diagonal elements relating longitudinal and translational or rotational DOFs.

Figure(s)

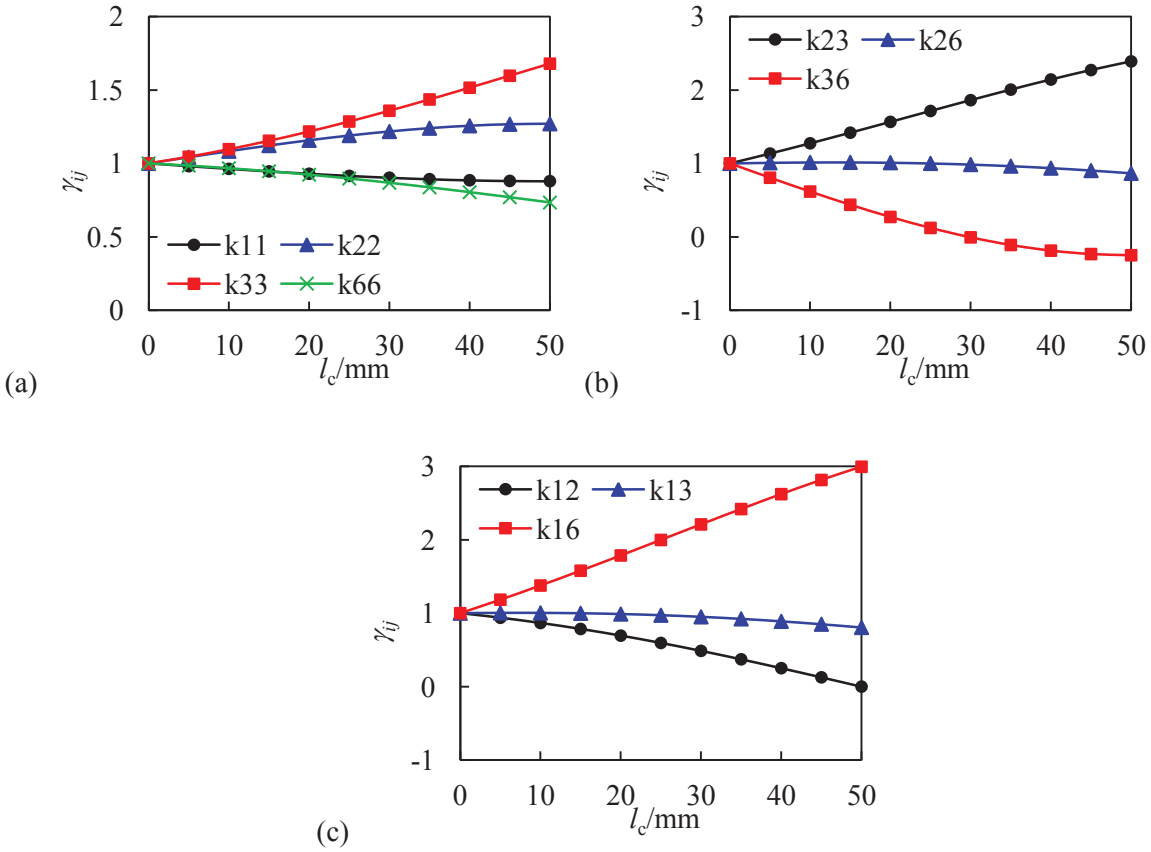

Fig. 7 Influence of crack location on the elements of stiffness matrix. (a) Diagonal elements; (b) Off-diagonal elements relating translational and rotational DOFs; (c) Off-diagonal elements relating longitudinal and translational or rotational DOFs.

Figure(s)

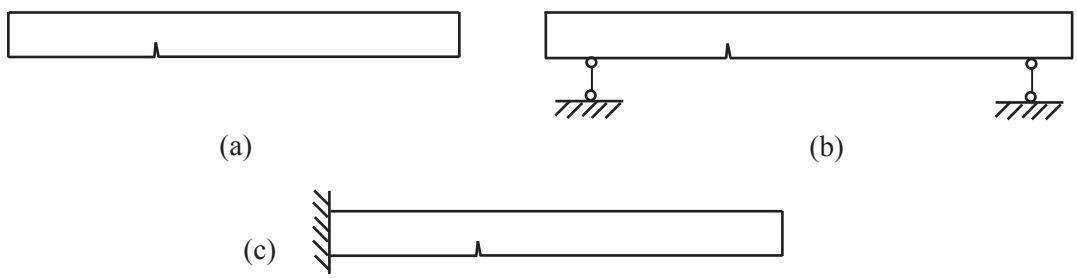

Fig. 8 Boundary conditions of the beams. (a) Free-free; (b) Simply supported; (c) Cantilever.

Figure(s)

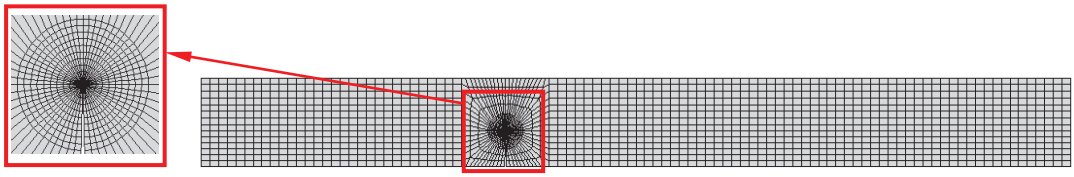

Fig. 9 Mesh of the FE model with solid elements

Figure(s)

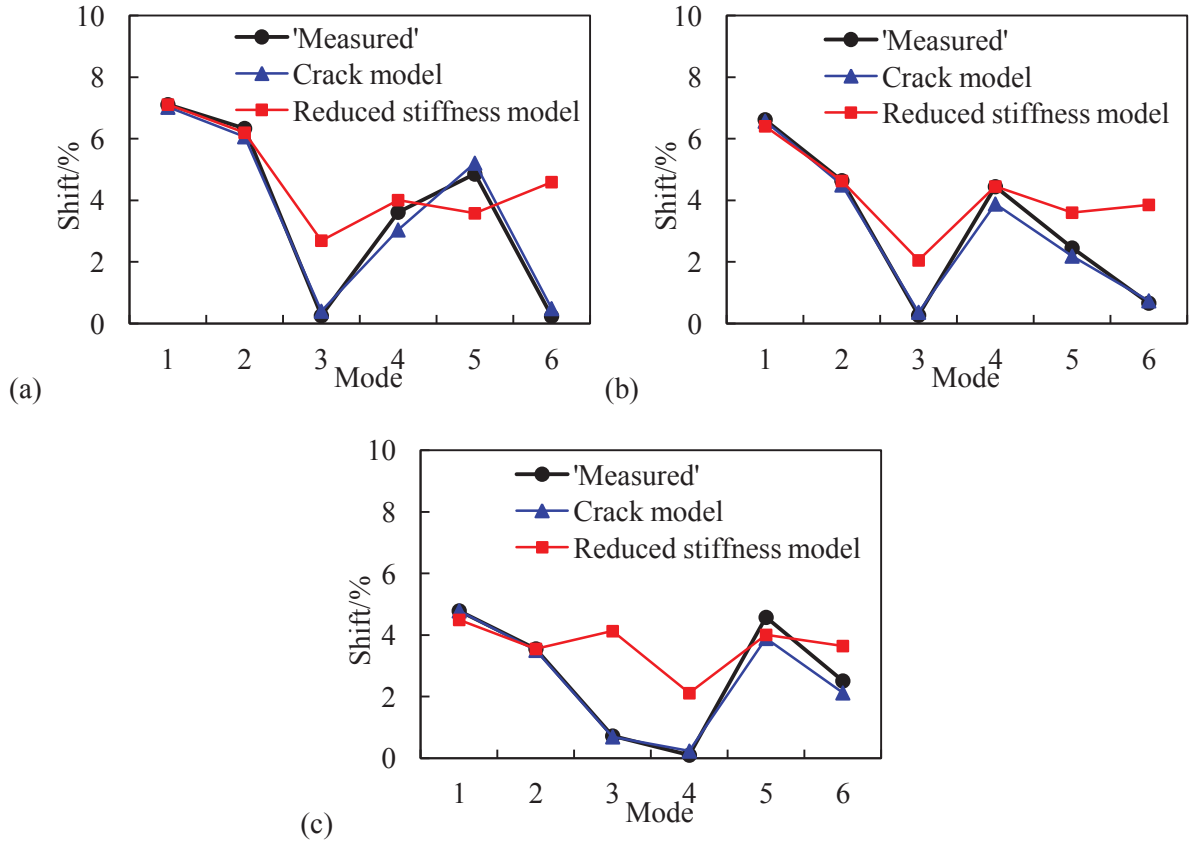

Fig. 10 Comparisons between ‘measured’ and predicted frequency shifts ($\alpha = 0.3$). (a) Free-free beam; (b) Simply supported beam; (c) Cantilever beam.

Figure(s)

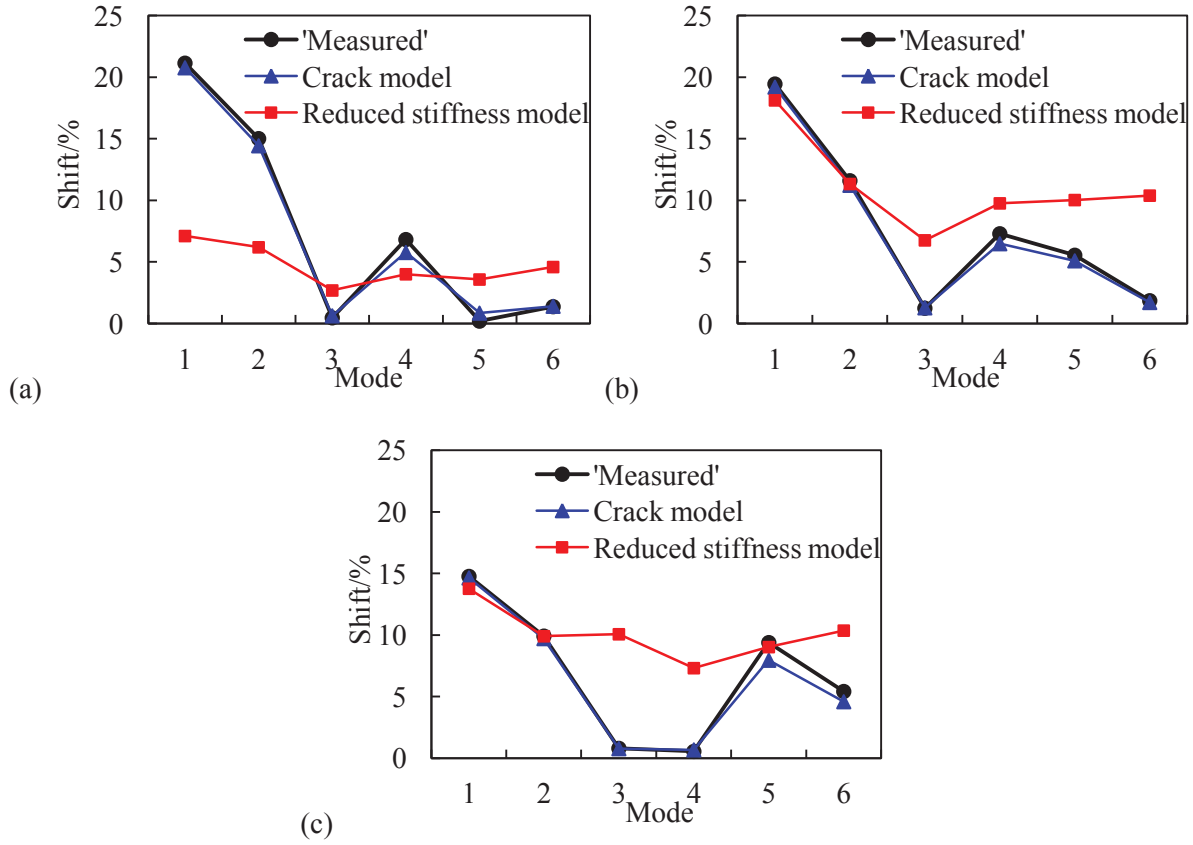

Fig. 11 Comparisons between 'measured' and predicted frequency shifts ($\alpha = 0.5$). (a) Free-free beam; (b) Simply supported beam; (c) Cantilever beam.

Figure(s)

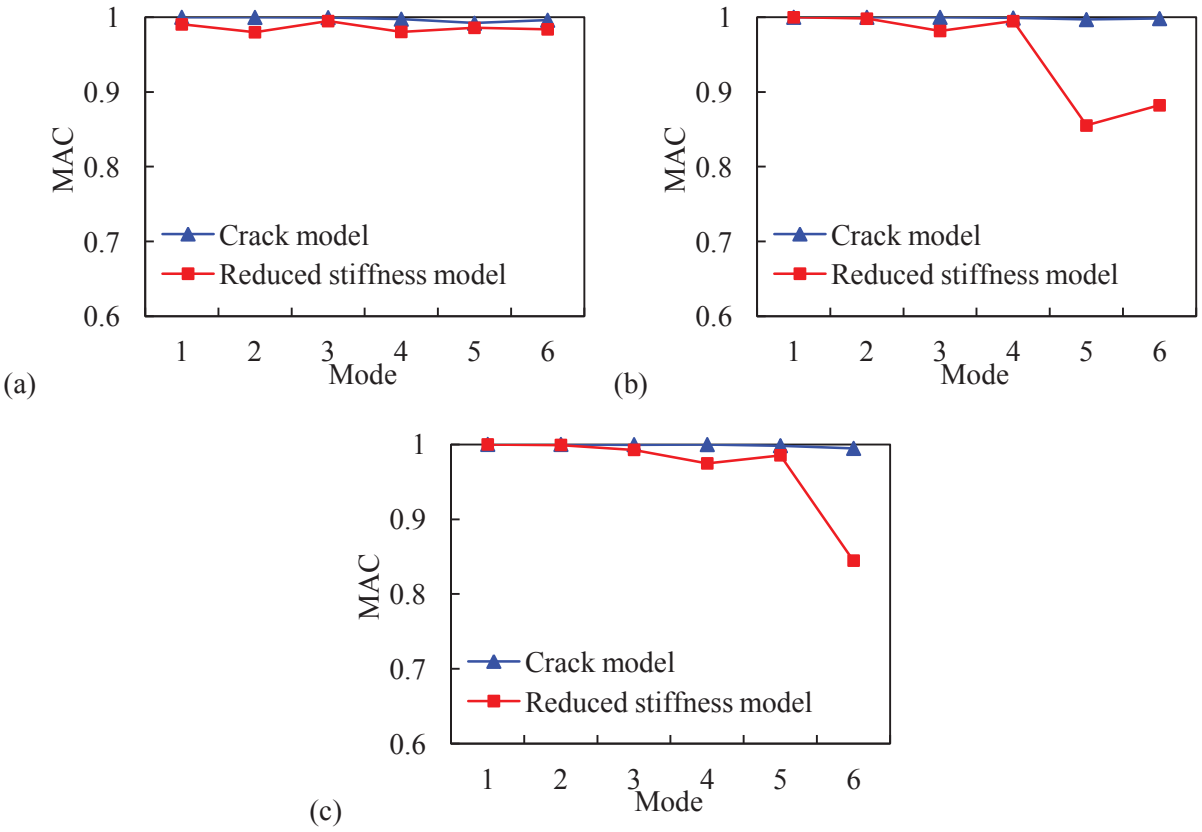

Fig. 12 Comparison between MAC results from two different models ($\alpha = 0.5$). (a) Free-free beam; (b) Simply supported beam; (c) Cantilever beam.

Figure(s)

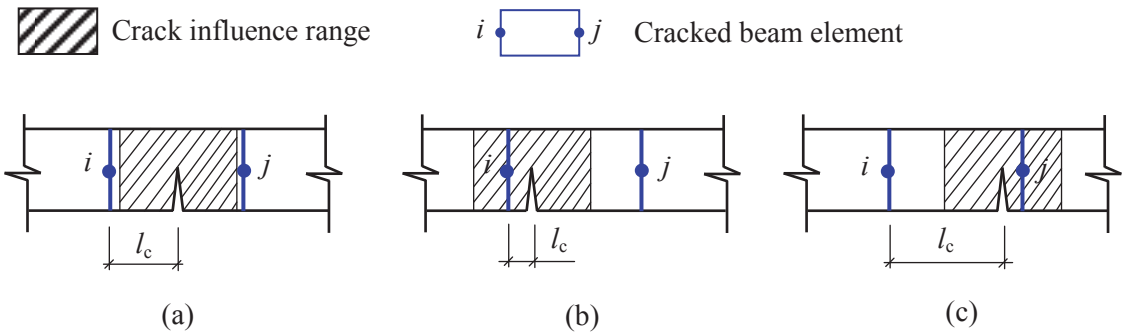

Fig. 13 Relationship between the crack influence range and the beam element. (a) Crack at element centre; (b) Crack close to left node; (c) Crack close to right node.

Figure(s)

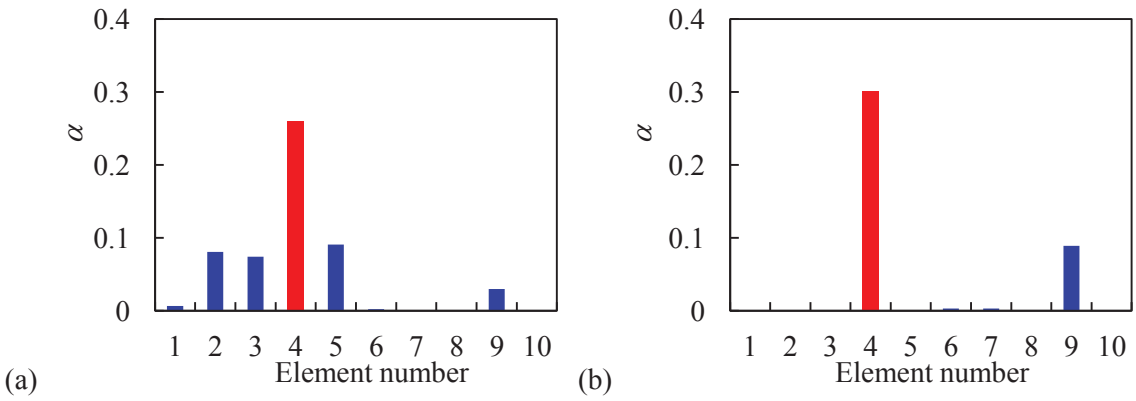

Fig. 14 Updating results of cantilever beam with $\alpha = 0.3$. (a) With 3 modes; (b) With 5 modes.

Figure(s)

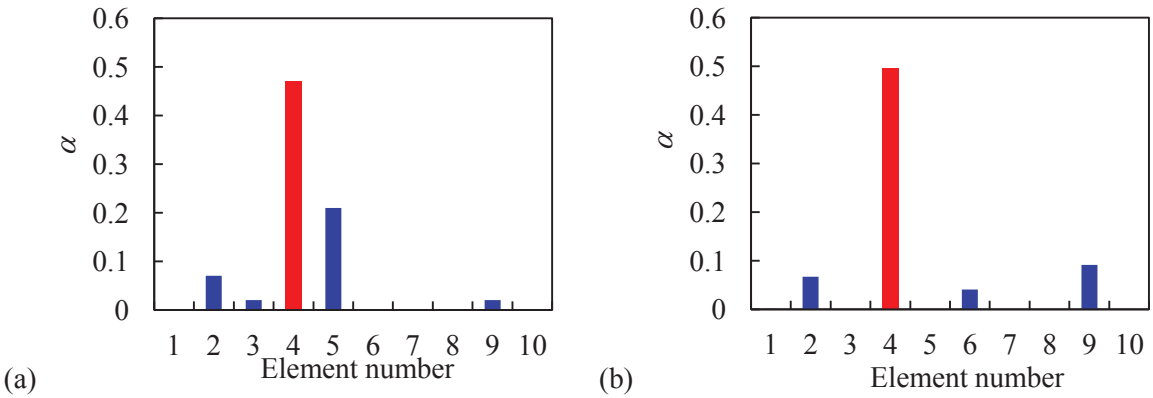

Fig. 15 Updating results of cantilever beam with $\alpha = 0.5$. (a) With 3 modes; (b) With 5 modes.

Figure(s)

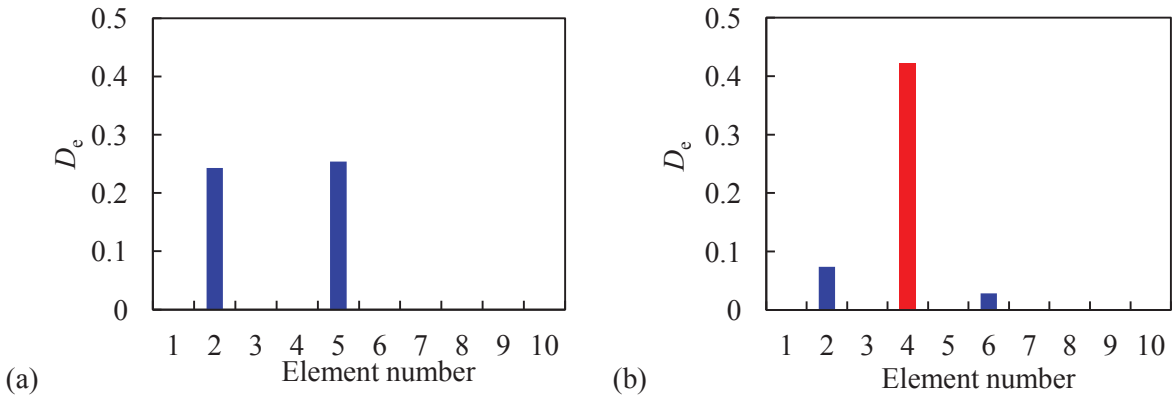

Fig. 16 Updating results of cantilever beam with $\alpha = 0.3$. (a) With 3 modes; (b) With 5 modes.

Figure(s)

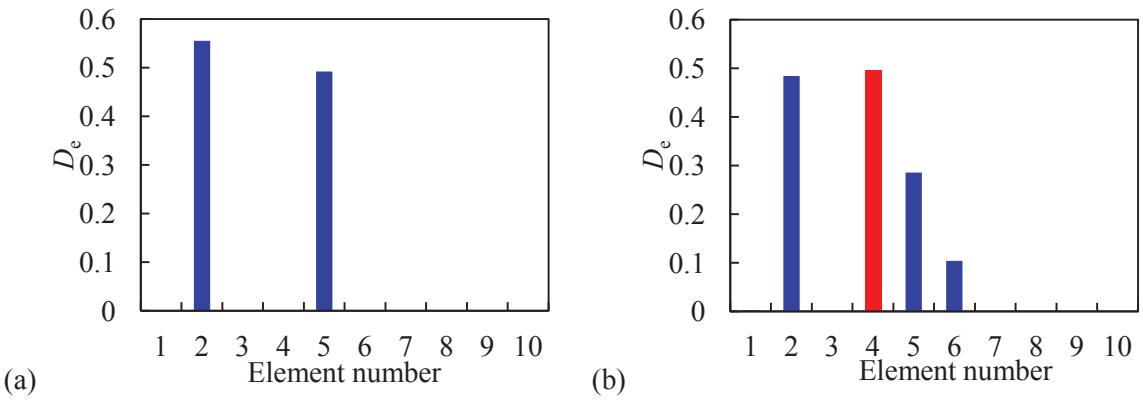

Fig. 17 Updating results of cantilever beam with $\alpha = 0.5$. (a) With 3 modes; (b) With 5 modes.

Figure(s)

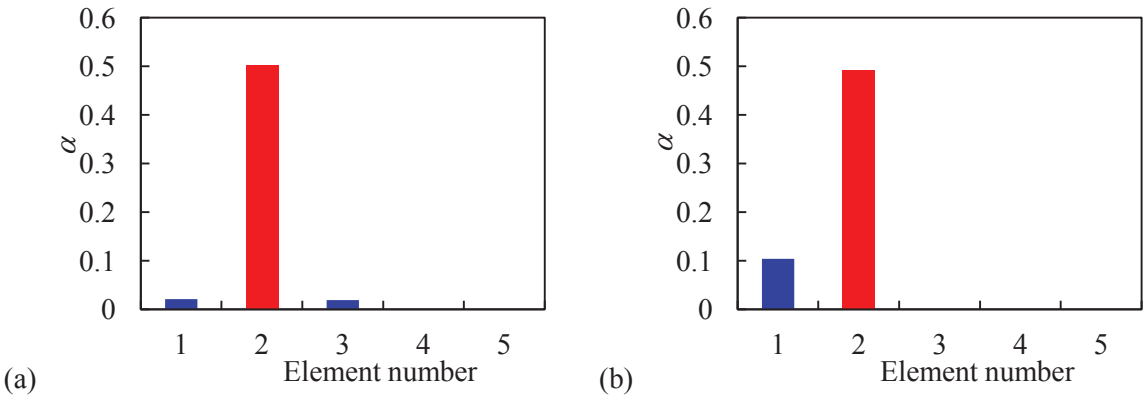

Fig. 18 Updating results of cantilever beam with $\alpha = 0.5$. (a) With 3 modes; (b) With 5 modes.

Figure(s)

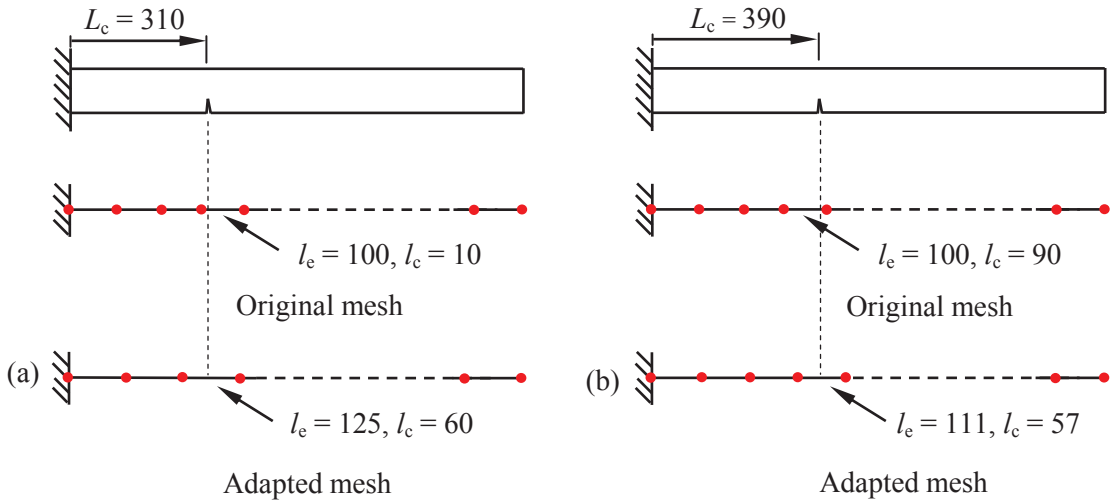

Fig. 19 Examples with adaptive updating strategy (Unit: mm). (a) Beam1; (b) Beam2.

Figure(s)

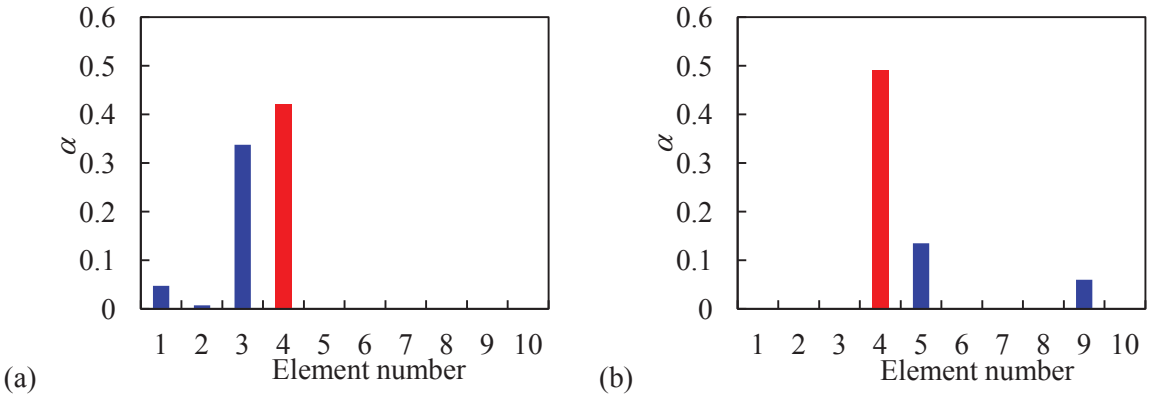

Fig. 20 Updating results of beams with non-centred crack. (a) Beam1; (b) Beam2.

Figure(s)

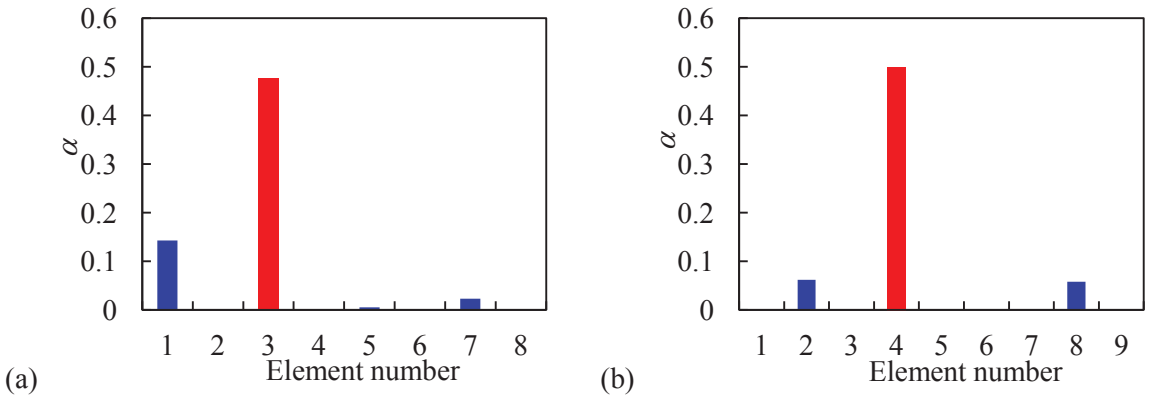

Fig. 21 Updating results with adapted mesh. (a) Beam1; (b) Beam2.

Figure(s)

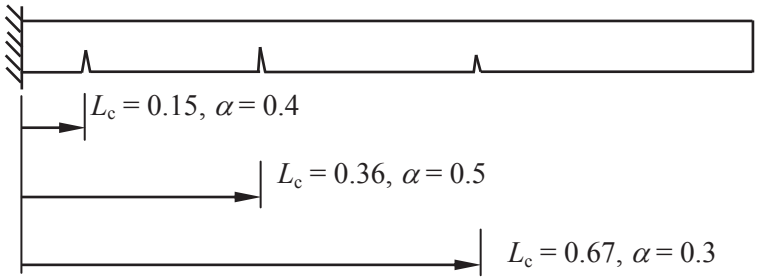

Fig. 22 Beam with multiple cracks

Figure(s)

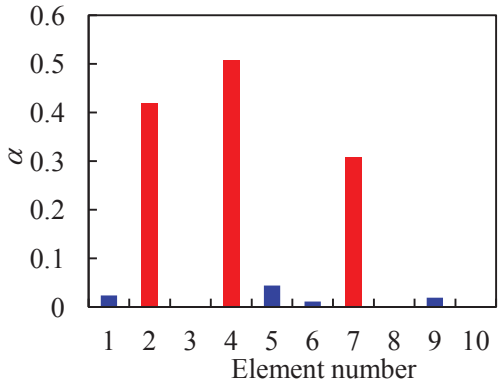

Fig. 23 Updating results of beam with multiple cracks